UNIVERSIDAD CARLOS III DE MADRID
SCHOOL OF ENGINEERING
AEROSPACE ENGINEERING DEPARTMENT

Low Thrust Collision Avoidance Manoeuvres

Bachelor Thesis

By

CARLOS ÁLVARO ARROYO PAREJO

Tutored and Supervised by

MANUEL SANJURJO RIVO

JUNE 2017

ABSTRACT

The present thesis is focused on the study of collision avoidance manoeuvres. It covers impulsive and low-thrust collision avoidance manoeuvres. Low-thrust collision avoidance is currently a important topic of research due to its current use in space missions and projects.

The thesis organisation presents in the first place a little introduction which covers the goals and motivation, and also includes a socio-economic and legal framework background related to this topic. There is also a state of the art which presents alternative studies related to collision avoidance manoeuvres and also exposes the latest fields of research of this issue.

The central part of the document summarizes the problem statement, the methodologies used to solve the problem and the different cases of study. This is the part where the problem of collision avoidance is explained and the different ways of solving the problem (absolute dynamics, relative dynamics and Keplerian propagation) are developed. In this way, the project is focused on explaining in detail each method and determine the assumptions required for each of them.

The final part includes the critical analysis of the results, a future work that can be carried out and the conclusions of the thesis, explaining the main important facts of the overall project.

DEDICATION AND ACKNOWLEDGEMENTS

I would like to dedicate this project in the first place to my family for all the effort and support they provided not only for me to continue my studies but for reaching what I have reached.

In the second place, I would like to dedicate my work to my tutor and supervisor Manuel Sanjurjo, for his constant support, dedication and the persistent guidance provided during the whole development of the thesis. Specially in those moments when nothing seemed to fit in.

Last but not least, I would like to dedicate my project to all my friends and classmates that helped me and from which I have learnt along my stay in the University. Guille, Christian, Gabriel, Iciar, Gemma, Álvaro, Jesús, Alberto, Javi, Iván, Dani, Patricia y Miguel. Thank you all.

"Just remember - when you think all is lost, the future remains." - Robert H. Goddard

AUTHOR'S DECLARATION

I declare that the work in this dissertation was carried out in accordance with the requirements of the University's Regulations and Code of Practice for Research Degree Programmes and that it has not been submitted for any other academic award. Except where indicated by specific reference in the text, the work is the candidate's own work. Work done in collaboration with, or with the assistance of, others, is indicated as such. Any views expressed in the dissertation are those of the author.

SIGNED: DATE: 21/06/2017

TABLE OF CONTENTS

Page

Abstract **ii**

Dedication and acknowledgements **iv**

Author's declaration **vi**

List of Tables **xi**

List of Figures **xiii**

Acronyms **xvi**

1 Introduction **1**

1.1 Background information 1
1.2 Socio-economic environment 3
1.3 Legal framework 4
1.4 Motivation 6
1.5 Project goals 7
1.6 Time planning 8
1.7 Budget 9
1.7.1 Human resources 9
1.7.2 Software cost 9
1.7.3 Hardware cost 9

2 State of the art **11**

2.1 Impulsive collision avoidance 12
2.2 Collision Probability 13
2.3 Low-thrust collision avoidance 15

3 Problem Statement **17**

4 Methodology **21**
4.1 Problem Geometry . . . 22
4.1.1 Position and velocity . . . 22
4.1.2 The b-plane . . . 25
4.1.3 Velocity impulse . . . 26
4.2 Keplerian propagation . . . 27
4.2.1 From orbital elements to state vector . . . 28
4.2.2 From state vector to orbital elements . . . 30
4.2.3 Steps followed in the Keplerian propagation . . . 32
4.3 Absolute dynamics . . . 34
4.3.1 Steps followed in the absolute dynamics . . . 35
4.4 Relative dynamics . . . 36
4.4.1 Steps followed in the absolute dynamics . . . 39

5 Cases of study **41**
5.1 Iridium-Cosmos collision . . . 42
5.2 Highly eccentric orbit . . . 45
5.3 Near head-on collision . . . 46

6 Results **47**
6.1 Keplerian propagation . . . 48
6.1.1 Iridium-Cosmos collision . . . 48
6.1.2 Highly eccentric orbit collision . . . 49
6.1.3 Near head-on orbit collision . . . 49
6.2 Absolute dynamics . . . 51
6.2.1 Impulsive manoeuvres . . . 51
6.2.1.1 Iridium-Cosmos collision . . . 51
6.2.1.2 Highly eccentric orbit collision . . . 52
6.2.1.3 Near head-on orbit collision . . . 52
6.2.2 Low thrust manoeuvres . . . 53
6.2.2.1 Iridium-Cosmos collision . . . 54
6.2.2.2 Highly eccentric orbit collision . . . 56
6.2.2.3 Near head-on orbit collision . . . 56
6.3 Relative dynamics . . . 57

6.3.1 Iridium-Cosmos collision 58
6.3.2 Highly eccentric orbit collision 58
6.3.3 Near head-on collision 59

7 Future work **61**

8 Conclusions **63**

Bibliography **65**

LIST OF TABLES

TABLE **Page**

1.1 Budget 10

5.1 Iridium-Cosmos collision geometry parameters [6]. 43
5.2 Iridium-Cosmos collision geometry additional orbital parameters. 44
5.3 Highly eccentric orbit collision geometry parameters [6]. 45
5.4 Near head-on collision geometry parameters [6]. 46

List of Figures

Figure **Page**

1.1 Population of space debris in the last 60 years 2
1.2 Annual space insurance claims resolved to date 4
1.3 Low-thrust collision avoidance manoeuvres. Project plan 2016-2017. 8

2.1 Evolution number of objects in LEO 14

4.1 Geometry of the problem with respect to a inertial reference frame <X,Y,Z>. 22
4.2 Geometric relation between $\mathbf{v_1}$ and $\mathbf{v_2}$ at the collision event 23
4.3 Geometry of the b-plane. Position, velocity and missdistance of S_1 and S_2 after the collision avoidance manoeuvre [6]. 25
4.4 ΔV manoeuvre geometry [6]. 27
4.5 Geometry of a general elliptic orbit [27]. 28
4.6 Geocentric equatorial fram and the orbital elements [9]. 29
4.7 Steps followed during Keplerian propagation 33
4.8 Steps followed applying absolute dynamics 36
4.9 Geometry of the relative motion [9]. 37
4.10 Steps followed applying relative dynamics 40

5.1 Iridium-Cosmos collision [19]. 42
5.2 Space debris released after Iridium-Cosmos collision [19]. 43
5.3 Optimal manoeuvre direction angles for Iridium-Cosmos collision [6]. 44
5.4 Optimal manoeuvre direction angles for highly eccentric collision [6]. 45
5.5 Optimal manoeuvre direction angles for near head-on collision [6]. 46

6.1 Iridium-Cosmos collision maximum miss distance [km] as a function of the manoeuvre change in the true anomaly. ΔV of 1 m/s. (Keplerian propagation) 48

6.2 Highly eccentric orbit collision maximum miss distance [km] as a function of the manoeuvre change in the true anomaly. ΔV of 1 cm/s. (Keplerian propagation) 49
6.3 Near head-on orbit collision maximum miss distance [km] as a function of the manoeuvre change in the true anomaly. ΔV of 1 cm/s. (Keplerian propagation) 50
6.4 Iridium-Cosmos collision maximum miss distance [km] as a function of the manoeuvre change in the true anomaly. ΔV of 1 m/s. (Absolute dynamics) . . 51
6.5 Highly eccentric orbit collision maximum miss distance [km] as a function of the manoeuvre change in the true anomaly. ΔV of 1 cm/s. (Absolute dynamics) 52
6.6 Near head-on orbit collision maximum miss distance [km] as a function of the manoeuvre change in the true anomaly. ΔV of 1 cm/s. (Absolute dynamics) . . 53
6.7 Iridium-Cosmos collision maximum miss distance as a function of the manoeuvre change in the true anomaly. Low-thrust manoeuvre (Absolute dynamics) 55
6.8 Highly eccentric collision maximum miss distance [km] as a function of the manoeuvre change in the true anomaly. T of 0.2 mN. (Absolute dynamics) . . 56
6.9 Near head-on collision miss distance [km] as a function of the manoeuvre change in the true anomaly. T of 10 mN. (Absolute dynamics) 57
6.10 Iridium-Cosmos collision maximum miss distance [km] as a function of the manoeuvre change in the true anomaly. ΔV of 1 m/s. (Relative dynamics) . . 58
6.11 Highly eccentric orbit collision maximum miss distance [km] as a function of the manoeuvre change in the true anomaly. ΔV of 1 cm/s. (Relative dynamics) 59
6.12 Near head-on orbit collision maximum miss distance [km] as a function of the manoeuvre change in the true anomaly. ΔV of 1 cm/s. (Relative dynamics) . . 59

Acronyms

LEO	Low Earth Obit
GEO	Geostationary Earth Orbit
RAAN	Right Ascension of the Ascending Node
ESA	European Space Agency
IADC	Inter-Agency Space Debris Coordination Committee
UN COPUOS	United Nations Committee on the Peaceful Uses of Outer Space
ACA	Active Collision Avoidance
PMD	Post-Mission Disposal
ADR	Active Debris Removal

CHAPTER 1

INTRODUCTION

In the last sixty years the threat of space debris has become more relevant in terms of space utilisation and collision between spatial systems and the space debris. This chapter is focused in exposing a background information related to historic collision events and space debris, and standing out the importance of collision avoidance in the last few years. Moreover, the socio-economic environment and the legal framework, where collision avoidance has a great impact, will be introduced. Particularizing, in this thesis, the motivation, goals and methodology of the project are going to be determined in order to highlight the issues of interest of the project. Finally, the time planning and budget for the project are explained.

1.1 Background information

The population of space debris in LEOs (Low Earth Orbit) and GEOs (Geosynchronous Earth Orbit) have been increasing in the last sixty years due to the great amount of space missions and operations.

According to ESA [10] since 1957 about 5250 rocket launches have been performed which implies that the number of space debris has experienced a continuous growth in these six decades as shown in Figure 1.1. This graph shows the growth of the different types of space debris during the last sixty years since 1957.

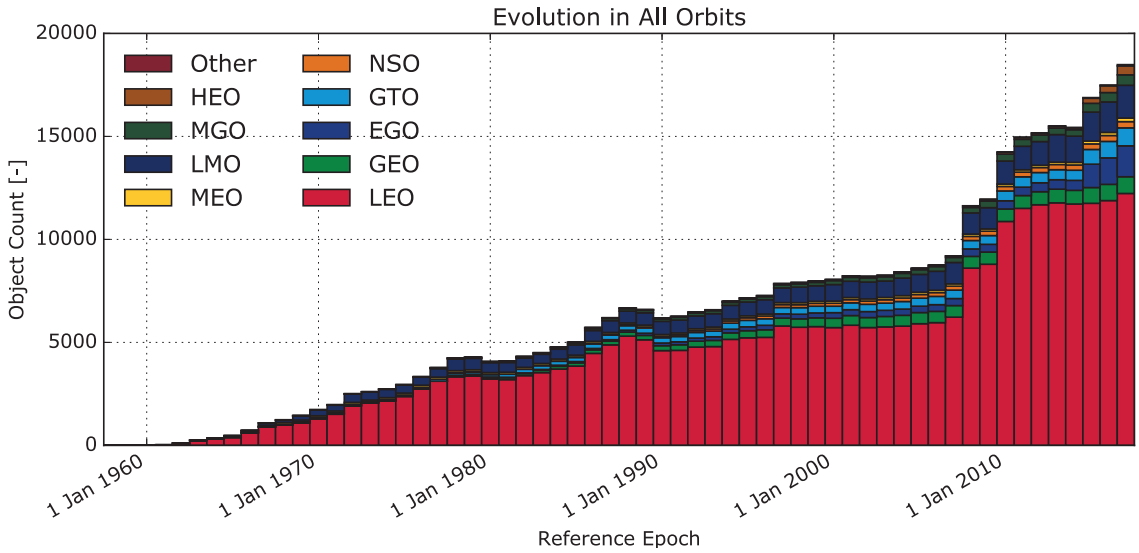

Figure 1.1: Population of space debris in the last sixty years [10].

The increment in the number of space debris has been the responsible of several collisions that could be avoided using collision avoidance manoeuvres. Ones of the most important collisions between spacecraft and orbital debris are [18]:

- The Soviet military anti-satellite (ASAT) Cosmos 248 collided with Cosmos-252 on 1 November 1968.
- On 23 December 1991 the Soviet military navigation system Cosmos-1934 was damaged and hit by space debris.
- The French microsatellite Cerise was hit and damaged by space debris which produced a sudden change in its attitude. The impact took place on 24 July 1996.
- Meteorological satellite DMSP-8531 was impacted on 17 January 2005 by space debris.
- On 11 January 2007 an anti-satellite test occurred in which the meteorological satellite Fengyun 1C was destroyed. This fact added more than 3000 spaces debris.
- The most important collision is the well know Iridium-Cosmos in which the American communication satellite, Iridium-33 collided with the Russian military satellite Cosmos-2251. The importance of the collision is double, since both Iridium-33 and Cosmos-2251, were destroyed and also more than 2300 fragments were released after the collision. This particular case will be shown later in order to determine

what would have been the optimal solution to avoid the collision between both satellites.

Due to the aforementioned accidents, it is necessary to provide ways of avoiding the collision of spacecraft with the different space debris allocated in Earth orbits. This is profitable in two ways: on the one hand, collision avoidance between a spacecraft or satellite and space debris assures the safety and proper functioning of the spacecraft, and on the other hand, collision avoidance ceases the continuous increment in the accumulation of space debris since the prevention of collision events is also related to the generation of more space debris.

The ESA carries out around 12 collision avoidance manoeuvres per year according to their data [11]. The last collision avoidance manoeuvre was performed on 25 January 2017 where ESA's Swarm-B satellite avoided the collision with space debris of Cosmos 375 which exploded after its launch on 30 October 1970.

1.2 Socio-economic environment

In Section 1.1, it is mentioned how the collision with space debris has been critical in several cases affecting the attitude of the spacecraft or even the total destruction of the satellite like in the Iridium-Cosmos case. Another important issue, related to these collisions is to determining how much is lost due to the destruction of the spacecraft. In other words, in this section a study will be performed on how much money is saved through collision avoidance manoeuvres.

According to Levin and Carroll [20] the cost of a catastrophic collision includes: on the one hand the loss of the spacecraft due to the collision. However, the possible damages produced by the space debris released from the crash also need to be taken into account. The average total loss caused by the catastrophic collision can be estimated on the order of $30 million. This quantity would be approximately the savings if collision avoidance manoeuvre would have been carried out. The losses from the damages occurred as a consequence of the space debris generated through the collision, add up to $200 million.

The collision with space debris is considered as a threat by public and private agencies. This risk is nowadays accounted together with pre-launch and launch phases of the

spacecraft. Figure 1.2 shows the money covered by the insurance agencies due to pre-launch, launch and on-orbit events like collision with space debris.

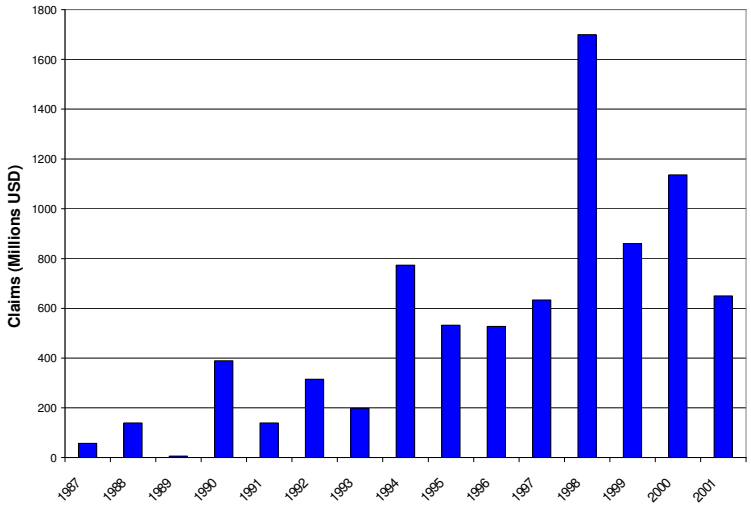

Figure 1.2: Annual space insurance claims resolved to date [12].

1.3 Legal framework

The existence of space debris is a problem that affects all nations in charge of space missions and space operations since space debris compromise the safety of the mission.

As it has been mentioned in Section 1.1, the accumulation of space debris has become relevant in the last sixty years. The improvement of the investigation on new ways to avoid or mitigate space debris, its understanding and the cooperation between different organizations and countries in order to provide improved databases, which contains all the space debris location and information, is closely associated to the increment of space debris accurate population.

In this pretext, international cooperation has become more relevant in the last few years. In 1993, the Inter-Agency Space Debris Coordination Committee (IADC), which is the most important international organization that deals with the problem of space debris, was founded. This entity provides several guidelines and recommendations in order to reduce the number of space debris per space mission or prevent the on-orbit collisions.

The principal guidelines are summarized in “IADC Space Debris Mitigation Guidelines" [17]:

- Limitation of debris released during normal operations.
- Minimisation of the potential for on-orbit break-ups.
- Post-mission disposal.
- Prevention of on-orbit collisions.

Each year, IADC is responsible of organizing several meetings where new ways of avoiding risk related to space debris are analysed and discussed. This agency is conformed by different countries: Germany, Italy, France, United Kingdom (and others of the European Union) , India, United States of America, China, Japan, Russia and Ukraine.

Apart from IADC, there are other two entities that are relevant in the legal activities related with space debris and the sustainability of space activities: the United Nations Committee on the Peaceful Uses of Outer Space (UN COPUOS) and International Standardisation Organisation - Subcommittee for Space Systems and Operations (ISO-TC20/SC14). This committees have gathered several guidelines related to space debris and based on the IADC Space Debris Mitigation Guidelines. They are collected in “Guidelines for the long-term sustainability of outer space activities”. This document contains 32 guidelines associated to space activities and the relevant ones for this project can be summarized in the following lines [8]:

- Adopt, revise and amend, as necessary, national regulatory frameworks for outer space activities.
- Supervise national space activities.
- Improve accuracy of orbital data on space objects and enhance the practice and utility of sharing orbital information on space objects.
- Promote the collection, sharing and dissemination of space debris monitoring information.
- Investigate and consider new measures to manage the space debris population in the long term.

1.4 Motivation

In the previous sections the importance of collision avoidance manoeuvres has been highlighted. The expenses related with collisions between spacecraft and space debris are very important issues when planning a new space mission and, although several guidelines have been promoted by different international organizations, nowadays there are a lot of things that need to be performed in order to assure the safety and the proper functioning of space operations. For this purpose, avoiding collisions with the so called space debris is compulsory. Moreover, since the 60's, the number of space missions have been growing and, therefore, the accumulation of space debris has been also incremented as a consequence. In terms of the solutions carried out, collision avoidance manoeuvres imply a good alternative to stop continued boosting in the number of space debris in GEOs but principally in LEOs.

Related to space debris mitigation, there are other alternatives that have been studied and analysed in the last few years, however these theories are not fully developed and need more time to be carried out: post-mission disposal (PMD) ot active debris removal (ADR). Thus, collision avoidance manoeuvres have had top relevance in recent years. Although collision avoidance manoeuvres have been investigated in different ways, it is important to provide new ways to support the previous assumptions and computations. Indeed, part of this project is devoted to validate the computations that have been developed in the last decade and provide alternative ways of computing the optimal collision avoidance manoeuvre.

Although the contribution of collision avoidance manoeuvres has become important in current space operations, mitigation of space debris has drawbacks. Collision avoidance manoeuvres allow to avoid collision with current space debris and, thus, avoid the generation of new space debris. However, it does not allow to remove the current debris orbiting in LEOs and GEOs and can be considered a patch more than a real solution to the problem of space junk.

Taking into account the current problem of space debris the importance of this project becomes relevant. As said before, one of the goals is to determine different ways to calculate a solution for the manoeuvres performed to avoid collision with space junk. Moreover, in the recent years the use of low-thrust engines in spacecraft has become

more common which implies that the previous analyses and studies, based on impulsive thrust engines, need to be changed. This project also covers this latter purpose and tries to determine if the previous studies can be directly applied in order to assure their reliability of and provide new formulations and solutions to determine the optimal collision avoidance manoeuvres.

1.5 Project goals

As referred in Section 1.4, the final goal of this project is to provide new ways of determining collision avoidance manoeuvres. In order to achieve this purpose, it is necessary to develop known theories and apply them in a first approach to the impulsive studies in order to check their viability and then, apply the theories focused on low-thrust engines. Based on the last statements, the project covers different ways to analyse the problem of low-thrust collision avoidance manoeuvres.

The main goals can be summarized in the following lines and they are ordered based on the time in which they have been performed in order to understand and verify the concepts learned during the project's development.

- Study and understand the importance of collision avoidance manoeuvres. Identify the requirements that have already been fulfilled and those that need to be reached.
- Define the absolute dynamics, relative dynamics and Kepler's orbital motion of collision avoidance manoeuvres based on impulsive thrust engines.
- Validate the theories proposed with previous results of different studies.
- Determine and apply the changes, if any, to the previous theories for the assumption of low-thrust engines.
- Compare both, impulsive and low-thrust results, for collision avoidance manoeuvres and make a critical analysis of the difference between the two models.

Besides these main goals, it is also important to outline the future work that can be carried out after this project and that will be explained in Chapter 7. Finally, the conclusions that have been reached during the development of the project are going to be pointed out in Chapter 8.

1.6 Time planning

In this section the schedule followed during the development of the project is shown in Figure 1.3. The project has been divided into several groups in order to define the tasks that have been performed:

- **Documentation.** These groups include the time dedicated to gather and understand the information related to the thesis.
- **Problem solving.** This part includes all the steps followed to analyse the problem and implement ways to solve it.
- **Thesis writing.** As a final point, the time dedicated to write the bachelor thesis.

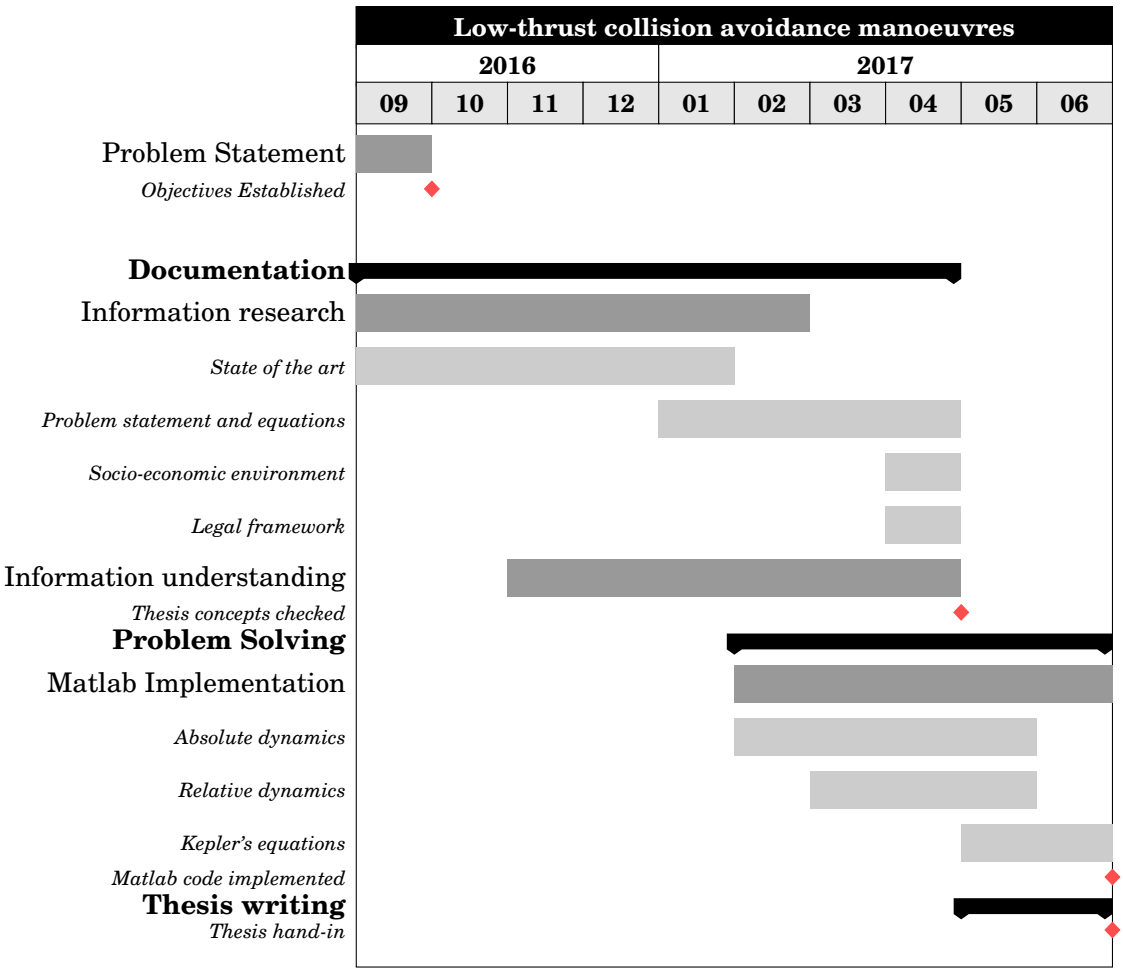

Figure 1.3: Low-thrust collision avoidance manoeuvres. Project plan 2016-2017.

1.7 Budget

The final section of this chapter correspond to all the costs associated to the bachelor thesis. The budget of any project is very relevant and needs to take into account taxes and depreciation since the beggining of the project, in order to provide a realistic cost. The budget proposed in this section does not represent precisely the real market price but it is a good approximation. The budget is divided in different types depending on the cost that is covered.

1.7.1 Human resources

Human resources takes into account the engineering salary based on the time dedicated to the bachelor thesis. In Article 33 of the Spanish "XVIII Convenio colectivo nacional de empresas de ingeniería y oficinas de estudios técnicos" [14] is gathered the minimum salary that a junior engineering must receive per year (maximum of 1800 working hours). This salary corresponds to 17,544.24€which gives 9.75 €/h. The minimum number of hours associated to the bachelor thesis are 300 hours (12 ECTS × 25 hour/ECTS). Thus, the human resources costs add up to a minimum of **2,925€**.

1.7.2 Software cost

The sotware part has been carried out by Matlab R2016b which has a license cost of 2,000€[1].Moreover, it can be also considered the operating system in which the software is implemented which is Windows 10 with a cost of 135€[2]. Thus, the software costs add up to **2,135€**.

1.7.3 Hardware cost

In terms of hardware, the main requirement has been the use of a laptop which has a cost of 700€. Assuming a depreciation period of 60 months and taking into account that the laptop has been used during the development of the bachelor thesis, the imputable cost can be estimated in **116.16€**.

[1]For this particular project it is only accounted the basic license. The information about this license and the rest of the products can be looked up in `https://es.mathworks.com/store/link/products/standard/new;jsessionid=c69663742e3edfd4febe7f53ce5e?s_iid=htb_buy_gtwy_cta1`

[2]The prices of Windows operating system license can be checked in the Microsoft Store `https://www.microsoftstore.com/store/mseea/es_ES/pdp/Windows-10-Home/productID.320437800?icid=CatPage-Win10-ModA-ShopNow-072916-MSEEA`

Finally, the cost are summarized in 1.1. Apart from the different types of cost aforementioned the VAT and indirect costs are also added to obtain the final total costs.

Human Resources					
Category		**Minimum number of hours**		**Total cost**	
Junior Engineering		300		2,925€	
Software					
Details		**Number of license**		**Total cost**	
Matlab R2016b		1		2,000€	
Windows 10		1		135€	
Hardware					
Details	**Quantity**	**Dedication (months)**	**Depreciation period (months)**	**Unity cost**	**Imputable cost**
Laptop	1	10	60	700€	116.16€
Total costs (without taxes)					5,176.16€
Indirect costs (15 %)					776.424€
VAT (21 %)					1,087€
TOTAL COSTS					**7,039.58€**

Table 1.1: Budget

CHAPTER 2

STATE OF THE ART

During the last decade the number of studies, analysis and projects related with collision avoidance manoeuvres have been incremented due to the concern about the sustainability of space. The sustainability of of LEOs and GEOs has been questioned in the last years due to the growth of space debris. In this way the new studies try to provide solutions that follow different ideas to stop the increment of space junk or even removing it. In this environment new solutions related to the mitigations of space junk have appeared. For instance post-mission disposal (PMD), active collision avoidance (ACA) manoeuvres of satellites or active debris removal (ADR) of obsolete satellites in orbit have been investigated. These new lines of study try to preserve the future of space sustainability and guarantee the success of future space missions.

The improvement of technology and the associated evolution of satellites and tracking systems have allowed to improve also the technical advance in space missions and collision avoidance. This improvement has also brought within a development in the propulsion system and increasingly new satellites are equipped with low thrust propulsion system. The problem rises up because these new technologies need to be validated with previous studies. The majority of the previous satellites and other spacecraft were equipped with impulsive propulsion systems and, in this sense, the reliability and applicability of previous studies need to be questioned due to the implementation of low thrusts propulsion systems.

The current chapter summarizes the previous studies of impulsive collision avoidance, the implementation of optimal solutions and the applicability of probability of collision to the calculation of the problem. It also gives some background information related to low-thrust collision avoidance projects carried out in different stages of space mission. Finally, the importance of this project is highlighted, taking into account the lack of information on the previous studies with respect to low-thrust collision avoidance manoeuvres.

2.1 Impulsive collision avoidance

Before starting the problem of low-thrust collision avoidance manoeuvres, it is important to take into account the previous studies and projects related with impulsive collision avoidance manoeuvres which are the grounds of this thesis.

One of the first analysis, which describes the problem of collision between two orbiting objects, is the one proposed by Akella and Alfried [1]. In this study the dynamic model of the collision is exposed and also the probability of impact. This document defines one of the best descriptions of the collision problem and has been taken into account in the next projects devoted to analyse the collision avoidance manoeuvres. Based on the idea of Akella and Alfried [1], Bombardelli [2] tries to determine a solution for different cases of study (which will be presented later in this project) from the perspective of impulsive collision avoidance manoeuvres. In this article, Bombardelli establishes the statement of the problem of the impulsive collision avoidance and exposes the kinematics and dynamics of the problem based on a different formulation than the one explained in this project: the generalized Pelaéz orbital elements [3, 26]. The analytical formulation of this problem is fully described also by Bombardelli [6] in which the description of the impulsive problem is again explained but pointing out the full description of the formulas and the Pelaéz orbital elements [3, 26].

The previous articles are very important to understand the problem of collision avoidance manoeuvres since they present several cases. In [2, 5, 6], the optimization of the impulsive problem based on the maximum possible miss distance achieved is also presented, i.e. the maximum change in the orbit geometry to avoid the impact with the space debris. The application of the velocity is different when the velocity impulse is applied in different directions of the trajectory. The kinematics and dynamics of the problem are presented, taking also into account the analysis of the space debris, since information is

gathered at the impact event when space debris and usable spacecraft collide.

The importance of the aforementioned documents is crucial since they provide the base in which this thesis is founded. The results obtained during their experiments will be compared in order to assure the formulation applied in this project. They are also the base of the problem understanding because they establish the problem statement and the steps followed to find the optimal solution. From this perspective, the present thesis try to find also the solution to the impulsive problem but applying a different formulation and methodology and also expect to find solution to the low-thrust collision avoidance problem.

Besides the analytic investigation, the direct application to real collision problems that have occurred in the space orbits also needs to be accounted. One example of this is suggested and explained in Luengo Cerrón et al. [24] which explains the different strategies and their implementation in the Deimos-1 and Deimos-2 satellites. In this particular case, it is remarkable, on the one hand, how collision avoidance manoeuvres take place in reality, and on the other hand, what are the steps that need to be followed in order to avoid the collision. During the procedure the importance of the predicted data is highlighted for several reasons. For instance, the data obtained through the tracking system allows to compute the evolution of the collision event depending on the location of the spacecraft and the space junk. Then the relative impulse that needs to be ordered to proceed with the manoeuvre is established and finally the trajectory prediction is calculated. This latter step needs to be reviewed since the final trajectory can let the satellite in a more dangerous position with respect to the space debris than before.

Moreover, on 25 January of 2017 the satellite Swarm-B which has a impulsive propulsion system formed by a cold gas propulsion subsystem was able to avoid a conjunction due to the calculations done at ESOC operations centre in Darmstadt, Germany. The satellite was going to collide with a space debris coming from the Cosmos 375 mission. The impulse given to the satellite was about 7-8 mm/s [28].

2.2 Collision Probability

The importance of collision probability come to light in terms of optimization. The problem optimal solution can be now determined following a different approach or adding

up to the solution the collision probability. In other words, the solution can now be expressed in three ways. The first solution is the one exposed in [2, 6] the problem is optimized trying to achieve the maximum possible miss distance. The second solution establishes that the optimum solution comes up when the minimum collision probability manoeuvre is performed [4, 5, 25]. And, finally, the comparison between both solutions can be made or even try to find the optimization allowing the maximum miss distance and the minimum collision probability.

Bombardelli et al. [5] implements the collision probability to the previous problem statement in order to obtain a solution when the minimum collision probability needs to be achieved. The solution obtained is very similar to the one obtained when the maximum miss distance manoeuvre is performed. The idea of the previous document is extended by Bombardelli and Hernando [4] in which the analytical formulation related to collision probability is improved and explained in depth. The results, as the previous ones, show the close relation between both optimizations. Due to this fact, the present thesis focuses on the miss distance optimization based on different analytical formulation.

This general solution can be applied and studied in LEO orbits where the probability collision is higher than in other orbits due to the accumulation of space debris in LEO, specially during the last decade (Figure 2.1). For this cases, the collision probability is obtained for different radii. And finally, a relation between the thrust required and the collision probability is obtained [25].

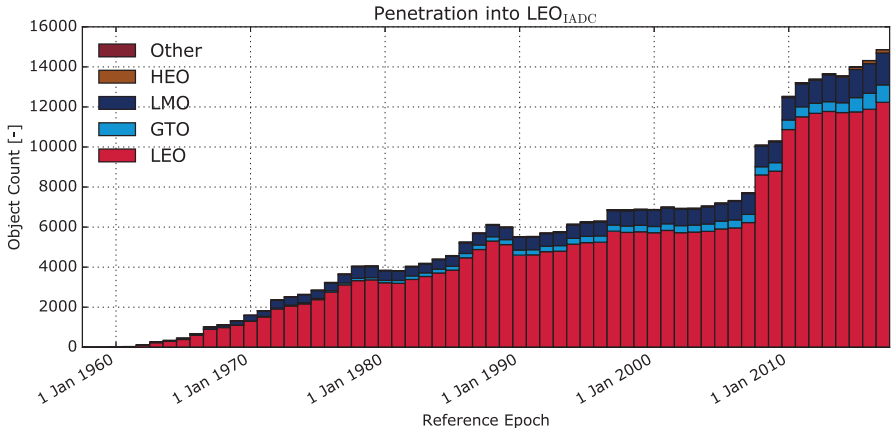

Figure 2.1: Evolution number of objects in LEO [10].

The exposed real case of Section 2.1 had also taken into account the collision probability. Through an iterative process and depending on the time that the manoeuvre needs to be performed, the actuation on the Deimos-I which gave a signal of two possible collision events is chosen. For this case, the probability of conjunction was calculated for both collision events and the subsequent avoidance manoeuvre depended on it [24].

2.3 Low-thrust collision avoidance

Regarding low-thrust propulsion systems, there are several works that have developed theories and applicable analysis to collision avoidance manoeuvres. A first approach to the problem of low-thrust is given in [13]. In this document the minimum thrust is associated to the time in which the manoeuvre is performed and it depends on the warning tracking system of the collision, being established in a maximum period of three days. The analysis is made in both LEO and GEO and takes into account the minimum thrust required for two types of impulsive thrusters.

Another work uses the low-thrust propulsion system in rendezvous guidance, providing ways of collision avoidance for this stage of a space mission [21]. In this case the parametrization of the problem is based on other algebraic formulation: the basis splines.

The low-thrust collision manoeuvres are also useful in spatial formation flight [23, 30]. In these particular cases, the configuration of the spatial formation is subjected to collision avoidance manoeuvres. The analysis of the low-thrust collision avoidance is regarding the deputy satellite and the changes in the formation with respect to the chief satellite are measured and analysed. For these examples the J2 effect is taken into account. These studies also make their own optimization process based on variables different from the ones mentioned in the previous lines.

As in Sections 2.1 and 2.2 there are studies whose fundamentals are based on real cases. In 2001 a collision avoidance manoeuvre was performed by the satellite CryoSat. As a consequence of this fact, there were some studies trying to determine if the manoeuvre could be performed following a low-thrust propulsion [15]. The collision avoidance manoeuvre for the CryoSat was analysed some days before its impact and in this case it was also determined the number of thrust arcs that need to be performed as well as the initial point at which the manoeuvre is carried out.

CHAPTER 3

PROBLEM STATEMENT

Before starting to develop the methodology and formulation followed to find the solution of the problem, it is necessary to state the problem that needs to be solved in a clear manner. The problem statement needs to gather the main objectives exposed in Section 1.5. According to this, the problem statement for a collision avoidance manoeuvre can be described as in [2]:

> *"Let us suppose a collision is predicted to occur between two satellites S_1 and S_2 within a time span Δt and let the satellite S_1 be set up to perform an avoidance ΔV manoeuvre of given magnitude along a chosen direction and time before the collision. What is the manoeuvre direction and instance that maximize the close-approach distance between the two objects?"*

As said before, the answer to this question needs to involve the main objectives established in Section 1.5. Moreover, there are several tasks that need to be performed in order to obtain the specific solution applied to low-thrust collision avoidance manoeuvres, not the general one. The steps that are going to be followed are also based on the ones stated by Bombardelli [2] and each step contributes to solve one of the main objectives of the problem.

1. Given the parameters of the collision event, determine (through the different analytical formulations) the dynamic state of both colliding objects, i.e. determine the position and velocity of both satellites at the conjunction event.

2. Implement, to the different analytical formulations, the parameters related to collision avoidance manoeuvres (impulse and low-thrust), i.e. determine the magnitude, direction and orbit location at which the velocity impulse is applied.

3. Solve the problem and analyse the results based on the maximum miss distance achieved depending on the different parameters implemented in step 2.

Besides the formulation of the collision avoidance problem, there are several parameters that are given in order to follow properly the previous steps and obtain, finally, the solution and the evolution of the maximum miss distance achieved. These parameters describe and allow to calculate two types of information. On the one hand, some parameters define the orbit geometry of the main satellite and the orbit location of both satellites at the impact event. On the other hand, the rest of the parameters are in charge of relating the velocity and their direction of both satellites and can also be used to determine the location of the b-plane. Both contribution of the parameters will be further explained in Chapter 4.

Although the meaning and formulation of the b-plane will be also defined in Chapter 4, it is important to mention it since the maximum achievable miss distance and its evolution will be presented in the b-plane as an easier way to analyse and visualize the results of the collision avoidance problem.

Once the function of the main parameters of the problem has been explained it is also important to mention them, to know how to proceed in the following chapters to find the solution. The main parameters established by the problem statement at the conjunction event are[1]:

- a_0. Semi-major axis of the orbit of the maneuverable satellite S_1. Given in km.

- e_0. Orbital eccentricity of the maneuverable satellite S_1.

[1]This parameters are gathered by Bombardelli in [2].

- ϕ. Rotating angle of the velocity of S_2 around the normal to S_1 orbital plane. Given in degrees.
- ψ. Out-of-plane rotating angle of the velocity of S_2 with respect to S_1 orbital plane. Given in degrees.
- θ_c. True anomaly of the orbit at the impact event of the maneuverable satellite S_1. Given in degrees.
- χ. Rescaling factor between the velocity of S_2 and S_1.

The problem statement is, finally, concluded and then, in order to solve it the methodology of Chapter 4 will be applied taking into account the parameters stated.

CHAPTER 4

METHODOLOGY

The problem of collision avoidance manoeuvres can be analysed from different perspectives and taking into account different analytical solutions. As mentioned in Chapter 2 one of the formulations is based on the generalized Pelaéz orbital elements [3, 26]. This is not the formulation that is going to be presented in this document due to the complexity of the understanding of the elements presented in the analytical solution. Although this formulation is not implemented in the present bachelor thesis, it is important to take it into account in order to check the reliability of the method and have a critical point of view when comparing the results.

This chapter tries to simplify the calculations and the understanding of the equations and steps to find out a solution for the collision avoidance problem. Due to this fact, the analytical formulation used during this thesis is founded on the basis of the orbital motion, i.e. the formulation presented is the basic formulation of orbital mechanics which is constituted by absolute dynamics of the two colliding objects with respect to a inertial reference frame centred in the Earth. The formulation is also associated to the relative motion between the two colliding objects being one of them the centre of the relative reference frame. Moreover, an analysis of the problem based on the Kepler's orbital elements, i.e. a change between the position and velocity vector determined in the collision event for both colliding objects and the classical orbital elements, is explained.

4.1 Problem Geometry

Given the problem statement and the initial parameters in Chapter 3, the geometry of the problem can be determined. Figure 4.1 shows the orbit of the maneuverable satellite with respect to a inertial reference <X,Y,Z> frame whose centre is supposed to be at the Earth. In this reference frame the X axis is located along the unperturbed orbit eccentricity. The Z axis will be orthogonal to the S_1 orbit plane and the Y complete the reference frame following the right-hand rule [25].

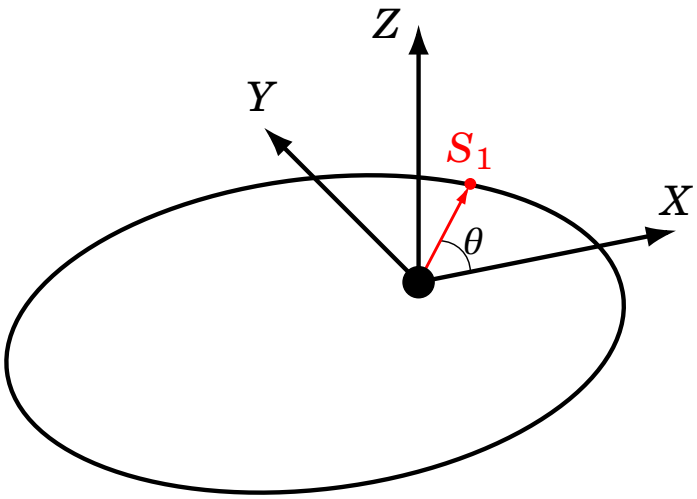

Figure 4.1: Geometry of the problem with respect to a inertial reference frame <X,Y,Z>.

At the conjunction event the true anomaly of the satellite will be the critical one given in the parameters $\theta = \theta_c$. Moreover the state vectors, i.e. the position and velocity vectors, can be determined by using the parameters of the problem with other parameters that correspond to the classical orbital elements and that will be defined in Section 4.2.

4.1.1 Position and velocity

Parting from the position and velocity vector of S_1 (the maneuverable satellite) at the conjunction event, it is possible to determine the position and velocity vectors of S_2 (the considered space debris). Obviously, the position vector with respect to the inertial reference frame <X,Y,Z> will be the same as for S_1. However, the velocity vector of S_2 needs a number of rotations, given the parameters of the problem, to be found [6]:

1. Rotate the velocity of S_1 by and angle $-\pi < \phi < \pi$ around the normal to S_1 orbital plane ($\mathbf{u_h}$).

2. Rotate the velocity with an out-of-plane angle $-\pi/2 < \psi < \pi/2$.

3. Finally, the magnitude of the vector is rescaled by a scale factor $\chi = \frac{v_2}{v_1}$, where v_2 and v_1 are the velocity magnitudes of S_2 and S_1 respectively.

In Figure 4.2 can be visualized the rotations explained in the previous steps which gives the geometric relation of $\mathbf{v_1}$ and $\mathbf{v_2}$.

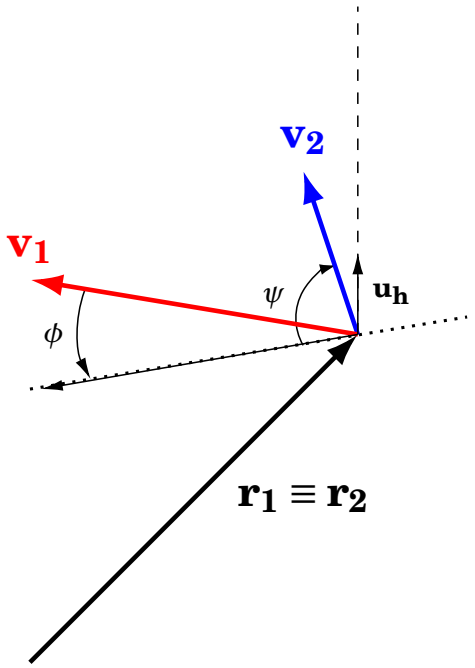

Figure 4.2: Geometric relation between $\mathbf{v_1}$ and $\mathbf{v_2}$ at the collision event

Given the geometric relation of the velocities of both satellites, the expression for the velocity of S_2 can be expressed as:

$$\mathbf{v_2} = \chi \left[\cos\phi\cos\psi\mathbf{v_1} - \sin\phi\cos\psi(\mathbf{v_1}\times\mathbf{u_h}) + v_1\sin\psi\mathbf{u_h}\right] \tag{4.1}$$

being

$$\phi = \text{atan2}[(\mathbf{v_1} \times \mathbf{v_2}) \cdot , \mathbf{v_1} \cdot \mathbf{v_2}] \tag{4.2}$$

$$\psi = \tan^{-1}\left[\frac{(\mathbf{v_2} \cdot \mathbf{u_h})\|\mathbf{v_2} \times \mathbf{u_h}\|}{v_2^2 - (\mathbf{v_2} \cdot \mathbf{u_h})^2}\right] \tag{4.3}$$

$$\chi = \frac{\|\mathbf{v_1}\|}{\|\mathbf{v_2}\|} \tag{4.4}$$

and where

$$\mathbf{u_h} = \frac{\mathbf{r_1} \times \mathbf{v_1}}{\|\mathbf{r_1} \times \mathbf{v_1}\|} \tag{4.5}$$

With this the Equation (4.1) can be expressed in terms of the inertial reference frame <X,Y,Z> as:

$$\mathbf{v_2} = \chi \begin{pmatrix} [v_{1,1}\cos\phi - v_{1,2}\sin\phi]\cos\psi \\ [v_{1,1}\sin\phi + v_{1,2}\cos\phi]\cos\psi \\ \|\mathbf{v_1}\|\sin\psi \end{pmatrix} \tag{4.6}$$

Besides the inertial reference frame <X,Y,Z>, another reference frame centred at the collision impact between S_1 and S_2 can be determined as <x,y,z>. In this new frame of reference there is one case which is excluded: if the velocities $\mathbf{v_1}$ and $\mathbf{v_2}$ are perfectly parallel. The new reference frame is considered unperturbed after the collision avoidance manoeuvre since the velocity of the collision avoidance manoeuvre is assumed to be negligible with respect to the orbital velocity of the maneuverable satellite. The directions of the new reference system can be formulated as [6]:

$$\mathbf{u_x} = \frac{\mathbf{v_1}}{\|\mathbf{v_1}\|} \tag{4.7}$$

$$\mathbf{u_z} = \frac{\mathbf{v_1} \times \mathbf{v_2}}{\|\mathbf{v_1} \times \mathbf{v_2}\|} \tag{4.8}$$

$$\mathbf{u_y} = \mathbf{u_z} \times \mathbf{u_x} \tag{4.9}$$

This new reference frame will allow to determine the b-plane and, subsequently, the change in position as a consequence of the collision avoidance manoeuvre on it.

Finally, before determining the function of the b-plane and the projection of the maximum miss distance, it is necessary to remark two assumptions related to the characteristics of the position and velocity before and after the collision avoidance manoeuvre. On the one

hand, the shift in the position of the maneuverable satellite at the conjunction event is considered small compared to the radial orbital distance and any change in the position due to an additional perturbation, apart from the velocity impulse, is considered to be negligible. On the other hand, the velocity of both satellites just before the conjunction event, i.e. for intervals of time $\Delta t \ll 1$, is considered as uniform rectilinear. In this way, the hypothesis called as short-term encounter condition [7] is assumed and the trajectories of the satellites can be represented as two straight lines in the <x,y> plane which collide at the impact event.

4.1.2 The b-plane

For the cases of study, the b-plane that it is going to be defined is the <ξ,η,ζ> b-plane reference frame centred for the cases on the space debris or the non-maneuverable satellite S_2 [29]. The different axis of the b-plane reference frame are: η axis oriented in the direction of the relative velocity between S_1 and S_2, ζ axis oriented in the opposite direction of the projection of the velocity $\mathbf{v_2}$ on the b-plane, and, finally, ξ axis completes the reference frame following the right-hand rule. The latter axis corresponds with the previous z axis. Moreover, in this axis the minimum orbit intersection distance (MOID) takes place. Figure 4.3 shows the representation of the b-plane and its reference frame.

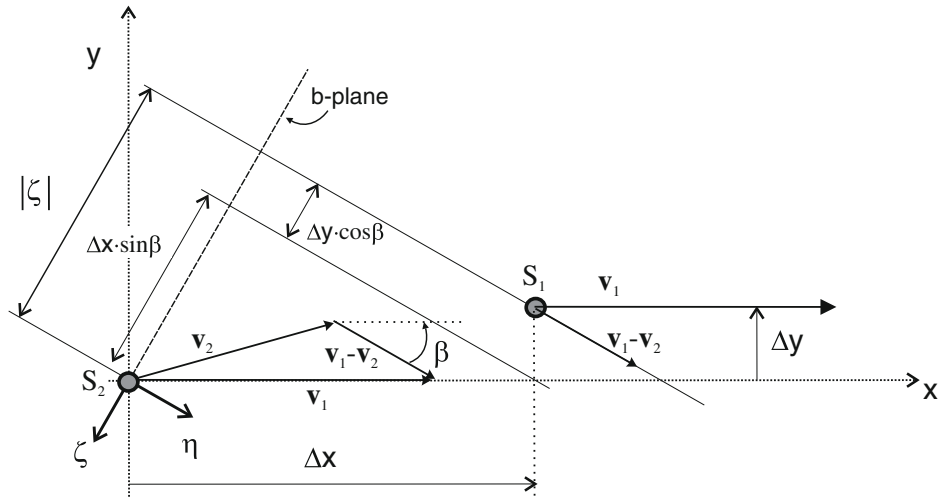

Figure 4.3: Geometry of the b-plane. Position, velocity and missdistance of S_1 and S_2 after the collision avoidance manoeuvre [6].

As stated before, the definition of the b-plane is used to understand and visualize in a better way the miss distance achieved through the collision avoidance manoeuvre. Taking into account that the shift in the position of S_1 as a consequence of the CAM in the <x,y,z> reference frame is <Δx, Δy, Δz>, in order to provide and expression for the maximum miss distance achieved in the b-plane, this shift must be projected in the b-plane reference frame as follows:

$$\xi = -\Delta z \tag{4.10}$$

$$\zeta = -\Delta x \sin\beta - \Delta y \cos\beta \tag{4.11}$$

where $\sin\beta$ and $\cos\beta$ can be defined as:

$$\cos\beta = \frac{(\mathbf{v_1} - \mathbf{v_2}) \cdot \mathbf{v_1}}{\|\mathbf{v_1}\| \, \|\mathbf{v_1} - \mathbf{v_2}\|} = \frac{1 - \chi \cos\psi \cos\phi}{\sqrt{1 - 2\chi \cos\psi \cos\phi + \chi^2}} \tag{4.12}$$

$$\sin\beta = \sqrt{1 - \cos^2\beta} \tag{4.13}$$

Finally, the maximum miss distance in the b-plane can be defined as:

$$\rho = \sqrt{\xi^2 + \zeta^2} \tag{4.14}$$

4.1.3 Velocity impulse

The last geometry that needs to be explained is the one related with the dynamics of the problem. In this case, the velocity impulse can be oriented in whatever direction and in the analytical formulation is applied in the radial, transverse and out-of-plane components. The velocity impulse for each component can be expressed as:

$$\Delta V_r = \Delta V \cos\gamma \sin(\sigma + \alpha) \tag{4.15}$$

$$\Delta V_\theta = \Delta V \cos\gamma \cos(\sigma + \alpha) \tag{4.16}$$

$$\Delta V_h = \Delta V \sin\gamma \tag{4.17}$$

where α is the flight path angle of the trajectory, σ is the in-plane rotation of the velocity and γ is the out of plane rotation (see Figure 4.4).

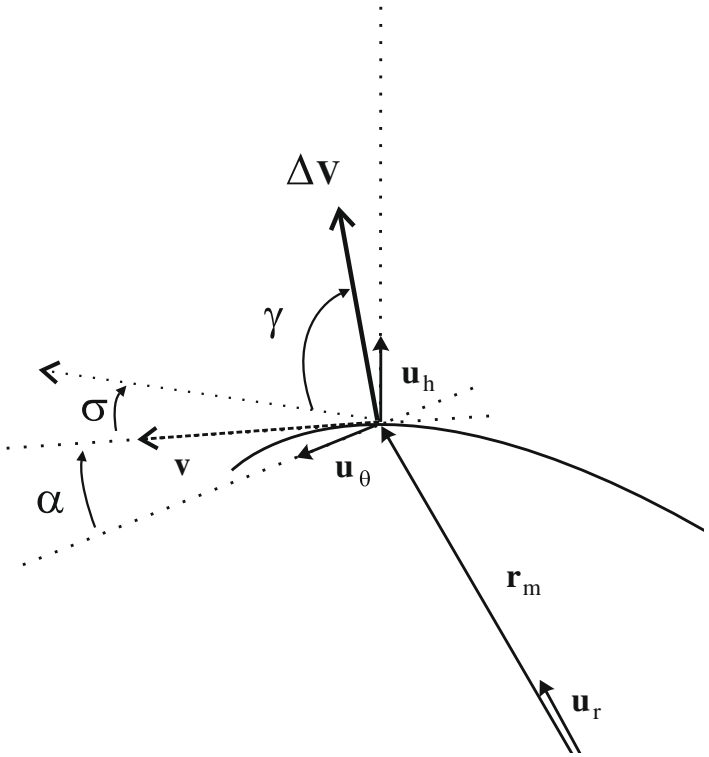

Figure 4.4: ΔV manoeuvre geometry [6].

In order to apply the velocity impulse not in this reference frame but in the <x,y,z>, the unitary vectors can be expressed as[1]:

$$\mathbf{u_h} = \frac{\mathbf{r_1} \times \mathbf{v_1}}{\|\mathbf{r_1} \times \mathbf{v_1}\|} \tag{4.18}$$

$$\mathbf{u_r} = \frac{\mathbf{r_1}}{\|\mathbf{r_1}\|} \tag{4.19}$$

$$\mathbf{u}_\theta = \frac{\mathbf{u_h} \times \mathbf{u_r}}{\|\mathbf{u_h} \times \mathbf{u_r}\|} \tag{4.20}$$

4.2 Keplerian propagation

In this part of the methodology the equations and steps followed to find the solution only for the impulsive manoeuvre are going to be developed. Some of the steps mentioned in here will also be used in the following sections.

[1]Remembering Equation 4.5

4.2.1 From orbital elements to state vector

The first step that needs to be done it is to determine the geometry of the orbit of the maneuverable satellite and the initial orbital parameters given in the problem statement to determine the state vectors of the satellite, i.e. position and velocity. In order to do so, the geometry of a general orbit is going to be shown and defined in Figure 4.5. From Chapter 3, the provided parameters are the eccentricity of the orbit, e, the true anomaly at the collision event, θ (f in the figure), and the semimajor axis a.

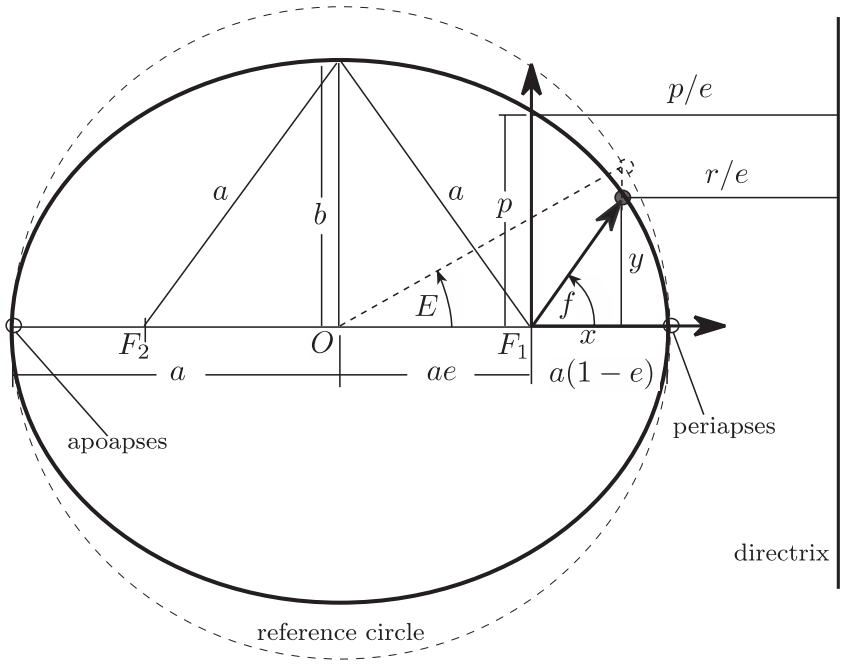

Figure 4.5: Geometry of a general elliptic orbit [27].

The parameter p of the figure is the semilatus rectum, defined as:

$$p = a(1-e^2) \tag{4.21}$$

With the previous expression and the geometry of the orbit the norm of the radius vector or, in other words, the modulus of the position of the satellite S_1 can be formulated as:

$$r = \frac{a(1-e^2)}{1+ecos\theta} = \frac{p}{1+ecos\theta} \tag{4.22}$$

The modulus of the velocity for an elliptic orbit can be obtained through the conservation of energy as described in [27]. Thus, it is described as:

$$v = \sqrt{\frac{2\mu}{r} - \frac{\mu}{a}} \tag{4.23}$$

where μ represents the standard gravitational parameter of the Earth.
In order to determine the components of the position and velocity vector at the impact event there are additional parameters that must be provided and that are not provided in the problem statement. These parameters correspond to other orbit elements of the problem and they are:

- Ω. Right ascension of the ascending node. Given in degrees.
- i. Inclination of the orbit. Given in degrees.
- ω. Argument of perigee. Given in degrees.

These parameters and the eccentricity and semimajor axis given in the problem statement, allow to determine the orbit location and its geometry with respect to the equatorial plane (see Figure 4.6).

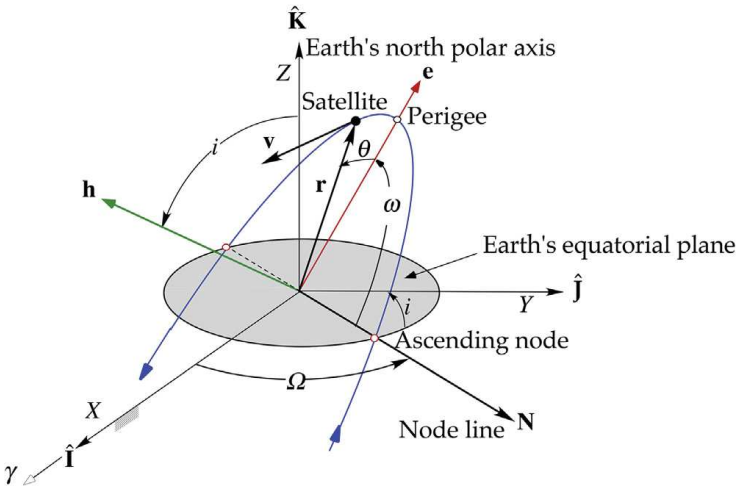

Figure 4.6: Geocentric equatorial fram and the orbital elements [9].

The component of the position vector **r** for the maneuverable satellite can be obtained by the Euler angle parametrization, i.e. the application of the different rotation matrix by the Euler angles which are the additional orbital elements stated before (ω, i, Ω). Thus,

$$x = r\left[\cos(\theta+\omega)\cos\Omega - \sin(\theta+\omega)\cos i\sin\Omega\right] \tag{4.24}$$

$$y = r\left[\cos(\theta+\omega)\sin\Omega + \sin(\theta+\omega)\cos i\cos\Omega\right] \tag{4.25}$$

$$z = r\left[\sin(\theta+\omega)\sin i\right] \tag{4.26}$$

In a similar way the components of the velocity vector **v** can also be determined as:

$$v_x = v\left[-\sin(\theta+\omega-\alpha)\cos\Omega - \cos(\theta+\omega-\gamma)\cos i\sin\Omega\right] \tag{4.27}$$

$$v_y = v\left[-\sin(\theta+\omega-\alpha)\sin\Omega + \cos(\theta+\omega-\gamma)\cos i\cos\Omega\right] \tag{4.28}$$

$$v_z = v\left[\cos(\theta+\omega-\alpha)\sin i\right] \tag{4.29}$$

where α is the flight path angle of the trajectory (also explained in Subsection 4.1.3) and can be determined as[2]:

$$\tan\alpha = \frac{e\sin\theta}{1+e\cos\theta} \tag{4.30}$$

With these equations, the conversion from orbital elements to state vectors **r** and **v** is achieved.

4.2.2 From state vector to orbital elements

In the previous subsection the computation of the state vector as a function of the orbital elements has been developed. In this section and also as a required step for obtaining the results, the opposite procedure is going to be developed: getting orbital elements parting from the state vector. For this purpose, some of the previous equations are going to be used but rearranging the terms in order to obtain the orbital elements. The calculation of the true anomaly θ it is not necessary since these parameters are going to be changed in order to get the evolution of the maximum miss distance as a function of the number of periods that the maneuverable satellite carries out, which is related to the true anomaly θ.

[2]The flight path angle of the trajectory α it is also given in the problem statement for certain cases. But, in order to make sense with the calculations of this thesis, it will be computed

The procedure that is going to be followed is similar to the one explained in [9]. Given the position **r** and velocity **v** vectors, its modulus can be easily determined applying the norm of each one. Next step is to calculate the angular momentum associated to the maneuverbale satellite:

$$\mathbf{h} = \mathbf{r} \times \mathbf{v} \;\; ; \;\; h = \|\mathbf{h}\| \tag{4.31}$$

Once the angular momentum is obtained the orbit inclination[3]

$$i = \cos^{-1}\left(\frac{h_z}{h}\right) \tag{4.32}$$

and the node line[4] (see Figure 4.6)

$$\mathbf{N} = \hat{\mathbf{K}} \times \mathbf{h} = \begin{vmatrix} \hat{\mathbf{I}} & \hat{\mathbf{J}} & \hat{\mathbf{K}} \\ 0 & 0 & 1 \\ h_x & h_y & h_z \end{vmatrix} \tag{4.33}$$

can be determined. The right ascension of the ascending node (RAAN) is calculated as:

$$\Omega = \begin{cases} \cos^{-1}\left(\dfrac{N_x}{N}\right) & \text{for } N_y \geq 0 \\ 360^\circ - \cos^{-1}\left(\dfrac{N_x}{N}\right) & \text{for } N_y \leq 0 \end{cases} \tag{4.34}$$

Since the eccentricity vector is necessary for the calculation of the argument of the perigee ω, it is going to be calculated and the eccentricity is just the modulus of the eccentricity vector:

$$\mathbf{e} = \frac{1}{\mu}\left[\times \mathbf{h} - \mu\frac{\mathbf{r}}{r}\right] \tag{4.35}$$

$$e = \|\mathbf{e}\| = \sqrt{1 + \frac{h^2}{\mu^2}\left(v^2 - \frac{2\mu}{r}\right)} \tag{4.36}$$

Thus, the argument of perigee is obtained as follows:

$$\omega = \begin{cases} \cos^{-1}\left(\frac{\mathbf{N}\cdot\mathbf{e}}{Ne}\right) & \text{for } e_z \geq 0 \\ 360^\circ - \cos^{-1}\left(\frac{\mathbf{N}\cdot\mathbf{e}}{Ne}\right) & \text{for } e_z \leq 0 \end{cases} \tag{4.37}$$

[3]The inclination angle i always take values from 0° to 180°.

[4]Note that $\hat{\mathbf{I}}$,$\hat{\mathbf{J}}$,$\hat{\mathbf{K}}$ are the unitary vectors of the inertial reference frame.

Besides the orbital elements, there are other parameters that are going to be used for the calculation of the miss distance and need to be mentioned. They are the orbital period, T, the eccentric anomaly, E, and the mean anomaly, M.

$$T = 2\pi\sqrt{\frac{a^3}{\mu}} \tag{4.38}$$

$$\tan\frac{E}{2} = \sqrt{\frac{1-e}{1+e}}\tan\frac{\theta}{2} \tag{4.39}$$

$$M = E - e\sin E \;\;;\;\; M - M_0 = \sqrt{\frac{\mu}{a^3}}\Delta t \tag{4.40}$$

finally, the conversion from state vectors to orbital elements is completed.

4.2.3 Steps followed in the Keplerian propagation

As aforementioned, the Keplerian propagation is going to be used only to check the reliability of the results of the impulsive manoeuvres. In order to get the results in terms of the miss distance several steps need to be applied. During these steps, the formulation exposed in the previous subsections is crucial and needs to be applied. The steps followed are:

1. Parting from the parameters of the problem statement, i.e. orbital elements, obtain the initial state vectors of the maneuverable satellite.

2. Propagate the problem backwards, i.e. change the true anomaly in n-periods, and obtain the new state vector at that location of the orbit.

3. Apply the velocity impulse in the tangential component of the velocity[5]. This step is made taking into account the velocity decomposition explained in Subsection 4.1.3.

4. With the new velocity vector $\mathbf{v}$, obtain the new orbital elements.

5. Propagate the problem forward the same number of periods as in step 2.

6. Calculate the difference in period produced by the change of orbital elements after applying the impulse velocity.

[5]According to [2], tangential component will be the optimal direction to apply the velocity impulse

7. Calculate the difference in the true anomaly. Look for the change in the mean anomaly, then for the change in the eccentric anomaly, and finally, the associated change in the true anomaly.

8. Calculate the position with the last orbital elements and due to the difference in the true anomaly.

9. Finally, the miss distance is calculated by the difference between the last position and the initial one calculated in step 1. The miss distance is projected onto the b-plane based on the explanation given in Subsection 4.1.2.

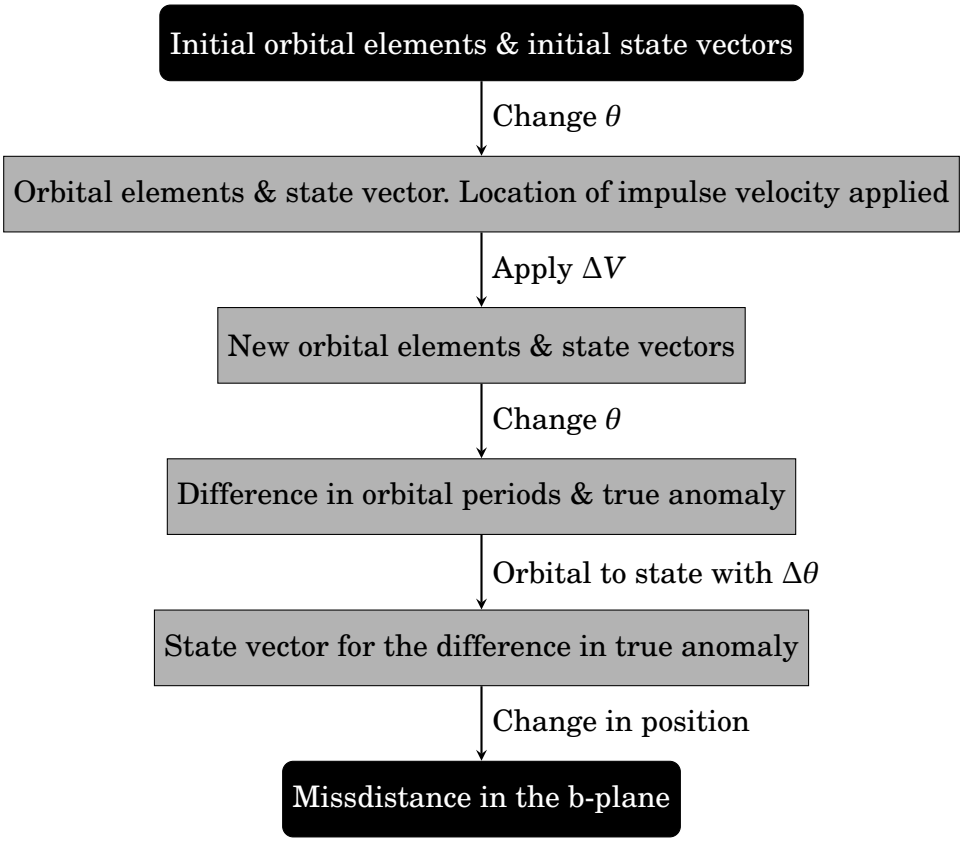

Figure 4.7: Steps followed during Keplerian propagation

4.3 Absolute dynamics

Another type of solution is given by the absolute dynamics. Different from the previous case the low-thrust manoeuvre can be analysed. This formulation is the basic one to determine position, velocity and acceleration of the maneuverable satellite or the space debris. In order to determine the state vectors, the formulation developed in the Keplerian propagation is going to be used. The calculation of the missdistance projected in the b-plane as well as the velocity impulse added at one point of the orbit location is also based in previous sections.

The first step is to determine the position vector of the manuverable satellite and the space debris at the impact event regarding that at this point both position vectors will be the same. The position vector will be expressed with respect to the the inertial reference frame <X,Y,Z> represented in Figure 4.1. Thus,

$$\mathbf{r} = X\hat{\mathbf{I}} + Y\hat{\mathbf{J}} + Z\hat{\mathbf{K}} \tag{4.41}$$

where $\hat{\mathbf{I}}$, $\hat{\mathbf{J}}$ and $\hat{\mathbf{K}}$ are the unitary vectors of the inertial reference frame <X,Y,Z>.

As stated in Subsection 4.2.3, the parameters of the problem statement are the characteristic orbital elements of the maneuverable satellite and the angles that relate the velocities of the satellite with the space debris at the conjunction event. Therefore, it will be necessary to convert the orbital elements to position vector following the same procedure as before.

Similarly, the velocity vector it is also determined by the conversion of the parameters of the problem statement. In terms of absolute dynamics the velocity vector is the derivative of the position vector such that:

$$\mathbf{v} = \dot{X}\hat{\mathbf{I}} + \dot{Y}\hat{\mathbf{J}} + \dot{Z}\hat{\mathbf{K}} = v_x\hat{\mathbf{I}} + v_y\hat{\mathbf{J}} + v_z\hat{\mathbf{K}} \tag{4.42}$$

Although the equations of position and velocity are useful in order to determine the geometry of the problem at the initial location, i.e. position and velocity vector at the impact event, the important parameter that needs to be formulated in terms of absolute dynamics is the acceleration.

Given the initial position and velocity of the problem, the acceleration needs to be integrated in order to determine the evolution of the maneuverable satellite. The acceleration of the maneuverable satellite with respect ot the inertial reference frame <X,Y,Z> is determined as:

$$\ddot{\mathbf{r}} = \mathbf{a} = -\frac{\mu}{r^3}\mathbf{r} \tag{4.43}$$

Equation (4.43) can be written in terms of the components of the acceleration:

$$\ddot{\mathbf{X}} = -\frac{\mu}{r^3}X \tag{4.44}$$

$$\ddot{\mathbf{Y}} = -\frac{\mu}{r^3}Y \tag{4.45}$$

$$\ddot{\mathbf{Z}} = -\frac{\mu}{r^3}Z \tag{4.46}$$

where r is the modulus of the position vector $\mathbf{r}$ and μ is the standard gravitational parameter for the Earth.

The main advantage of this formulation is that it is simple and easy to implement. It is also easy to visualize the evolution of the orbit with respect to the Earth given the initial position and velocity of the problem.

4.3.1 Steps followed in the absolute dynamics

In order to apply this formulation to the cases of study it is necessary to follow several steps as for the Keplerian propagation. The steps followed are:

1. Parting from the parameters of the problem statement, i.e. orbital elements, obtain the initial state vectors of the maneuverable satellite.

2. Integrate the problem backwards, given the initial conditions at the impact event. The integration time is the orbital period of Equation (4.38), which is also based on the change of true anomaly desired, $\Delta\theta$.

3. Applied the velocity impulse. This steps is made taking into account the velocity decomposition explained in Subsection 4.1.3. This step is skipped for low-thrust collision avoidance manoeuvres.

4. Integrate the equation forward, the same amount of time than step 2, taking into account the new initial conditions imposed with the addition of the velocity impulse ΔV. For low-thrust collision avoidance manoeuvres in the integration is implemented a typical thrust depending on the case of study and the mass of the maneuverable satellite.

5. Finally, the missdistance is calculated by the difference between the last position of the maneuverable satellite and the initial one calculated in step 1. The missdistance is projected into the b-plane based on the explanation given in Subsection 4.1.2.

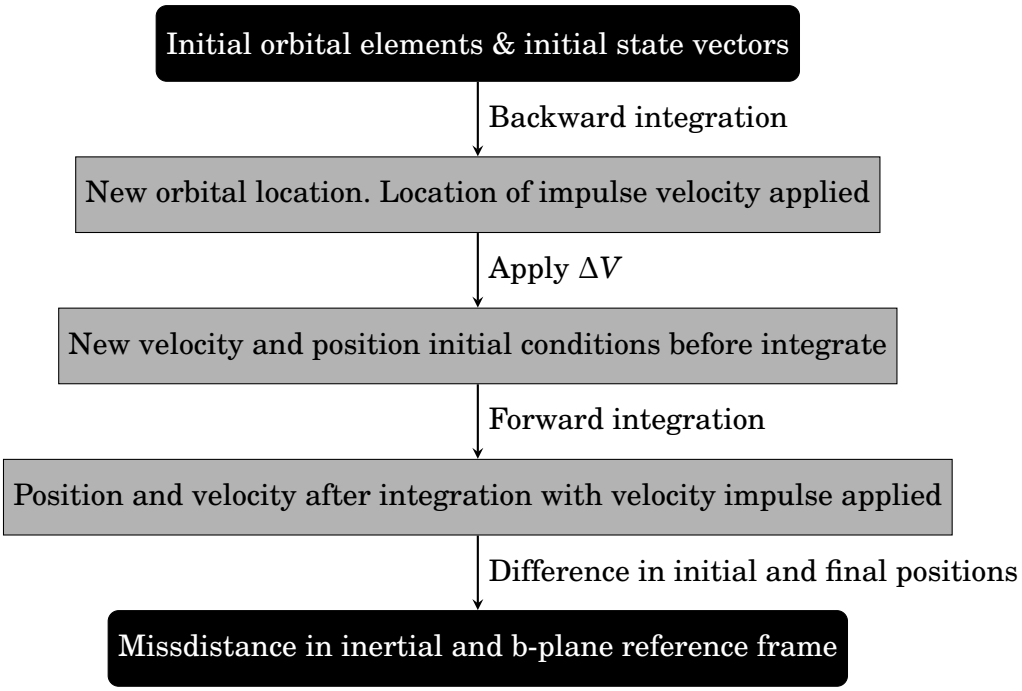

Figure 4.8: Steps followed applying absolute dynamics

4.4 Relative dynamics

This part of the methodology covers the formulation related to the relative dynamics. For this part there will be also some equations from previous sections that are going to be used. In this case two reference frame are established, one of them being a inertial reference frame. As in the previous case the conversion from orbital elements to state vectors is going to be used as well as all the equations needed to add the velocity impulse

and the equations needed to project the miss distance in the b-plane.

The first step is to define the system of reference for each satellite/space debris. In this case, the maneuverable satellite position vector is expressed with respect to an inertial reference frame <X,Y,Z> centred at the Earth as in Section 4.3. For the case of space debris it is necessary to define a moving reference frame centred in this case in the maneuverable satellite. Let <x,y,z> the moving reference frame centred at the satellite with unitary vector $\hat{\mathbf{i}}$, $\hat{\mathbf{j}}$ and $\hat{\mathbf{k}}$. The position vector of the space debris with respect to the moving reference frame is denoted as $\delta\mathbf{r}$. The geometry of the problem is shown in Figure 4.9.

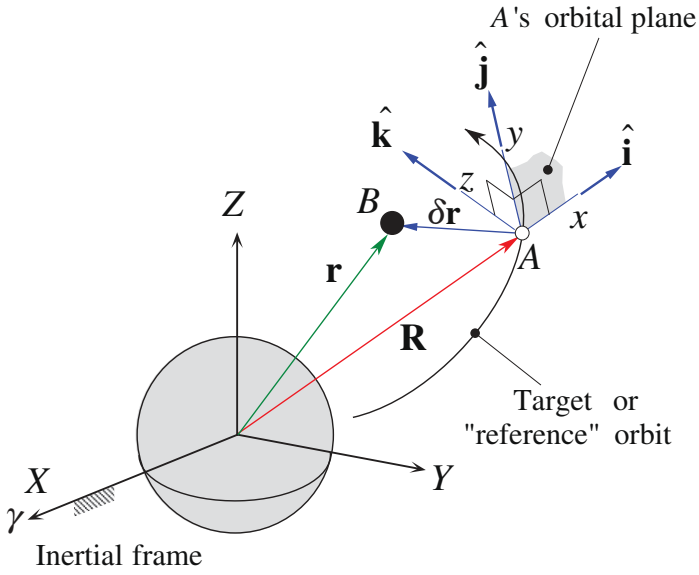

Figure 4.9: Geometry of the relative motion [9].

In the present geometry the maneuverable satellite equations are defined as in the previous section using Equations (4.41, 4.42, 4.43). The space debris geometry with respect to the inertial reference frame can also be formulated using these equations, however for the purpose of this section the relative motion is determined. As said before the relative position of the space debris with respect to the moving reference frame centred at the maneuverable satellite is given by:

$$\delta\mathbf{r} = \delta x\hat{\mathbf{i}} + \delta y\hat{\mathbf{j}} + \delta z\hat{\mathbf{k}} \tag{4.47}$$

The relative acceleration of the space debris can be expressed according to the geometry of the problem as [9]:

$$\delta\ddot{\mathbf{r}} = -\frac{\mu}{R^3}\left(-2\delta x\hat{\mathbf{i}} + \delta y\hat{\mathbf{j}} + \delta z\hat{\mathbf{k}}\right) \tag{4.48}$$

In this case the relative acceleration of the space debris with respect to the maneuverable satellite is measured in the inertial reference frame.

On the other hand, let $\delta\mathbf{a}_{\text{rel}}$ the relative acceleration with respect to the moving reference frame:

$$\delta\mathbf{a}_{\text{rel}} = \delta\ddot{\mathbf{r}} - \dot{\Omega}\times\delta\mathbf{r} - \Omega\times(\Omega\times\delta\mathbf{r}) - 2\Omega\times\delta\mathbf{v}_{\text{rel}} \tag{4.49}$$

Following a procedure similar to [9], the relative acceleration with respect to the moving reference frame can be formulated as:

$$\begin{aligned}\delta\mathbf{a}_{\text{rel}} = \delta\ddot{x}\hat{\mathbf{i}} + \delta\ddot{y}\hat{\mathbf{j}} + \delta\ddot{z}\hat{\mathbf{k}} = &\left[\left(\frac{2\mu}{R^3} + \frac{h^2}{R^4}\right)\delta x - \frac{2(\mathbf{V}\cdot\mathbf{R})h}{R^4}\delta y + 2\frac{h}{R^2}\delta\dot{y}\right]\hat{\mathbf{i}} \\ &+ \left[\left(\frac{h^2}{R^4} - \frac{\mu}{R^3}\right)\delta y + \frac{2(\mathbf{V}\cdot\mathbf{R})h}{R^4}\delta x - 2\frac{h}{R^2}\delta\dot{x}\right]\hat{\mathbf{j}} \\ &- \frac{\mu}{R^3}\delta z\hat{\mathbf{k}}\end{aligned} \tag{4.50}$$

Equation (4.50) can be separated into three scalar equations. Note that in order to obtain the relative position coordinates with respect to the moving reference frame the set of linear second order differential equations need to be solved. This set of differential equations is more useful than Clohessy-Wiltshire equations [9] since they not only take into account the assumption of circular orbits. In this equations the position in the x and y directions are coupled, and the position of the z axis on the moving reference frame is independent. The set of scalar linear second order differential equation can be formulated as follows:

$$\delta\ddot{x} - \left(\frac{2\mu}{R^3} + \frac{h^2}{R^4}\right)\delta x + \frac{2(\mathbf{V}\cdot\mathbf{R})h}{R^4}\delta y - 2\frac{h}{R^2}\delta\dot{y} = 0 \tag{4.51}$$

$$\delta\ddot{y} + \left(\frac{\mu}{R^3} - \frac{h^2}{R^4}\right)\delta y - \frac{2(\mathbf{V}\cdot\mathbf{R})h}{R^4}\delta x + 2\frac{h}{R^2}\delta\dot{x} = 0 \tag{4.52}$$

$$\delta\ddot{z} + \frac{\mu}{R^3}\delta z = 0 \tag{4.53}$$

As said before, these formulas allow to implement elliptic orbits to the calculation of the relative position in the moving reference frame. For a normal integration the angular momentum will remain constant and the vectors **R** and **V** will change (these are de position and velocity vectors of the maneuverable satellite in the inertial reference frame). When the velocity impulse is applied, this vectors and also the angular momentum h will change modifying the equations.
The important fact in this formulation is that the relative position vector $\delta\mathbf{r}$ obtained during the steps applied, will be directly the maximum missdistance achieved when the collision avoidance manoeuvre is performed. In this sense, although the formulation of the problem is complex, the solution to the problem seems to be easier to understand.

4.4.1 Steps followed in the absolute dynamics

The steps followed during the relative dynamics are very similar to those mentioned in Subsection 4.3.1. The steps followed are:

1. Parting from the parameters of the problem statement, i.e. orbital elements, obtain the initial state vectors of the maneuverable satellite.

2. Integrate the problem backwards, given the initial conditions at the impact event. The integration time is the orbital period of Equation (4.38), which is also based on the change of true anomaly desired, $\Delta\theta$.

3. Apply the velocity impulse. This step is made taking into account the velocity decomposition explained in Subsection 4.1.3. For this formulation the velocity impulse will change the velocity of the maneuverable satellite and that associated to the space debris. For low-thrust collision avoidance manoeuvres this step is skipped.

4. Integrate the equation forward, the same amount of time than step 2, taking into account the new initial conditions imposed with the addition of the velocity impulse ΔV. As for absolute dynamics, in this step the a characteristic thrust for each case of study and the mass of the satellite is added when applying the integration.

5. Obtain the relative position vector which correspond to maximum missdistance. Projected this vector in the b-plane based on the explanation given in Subsection 4.1.2.

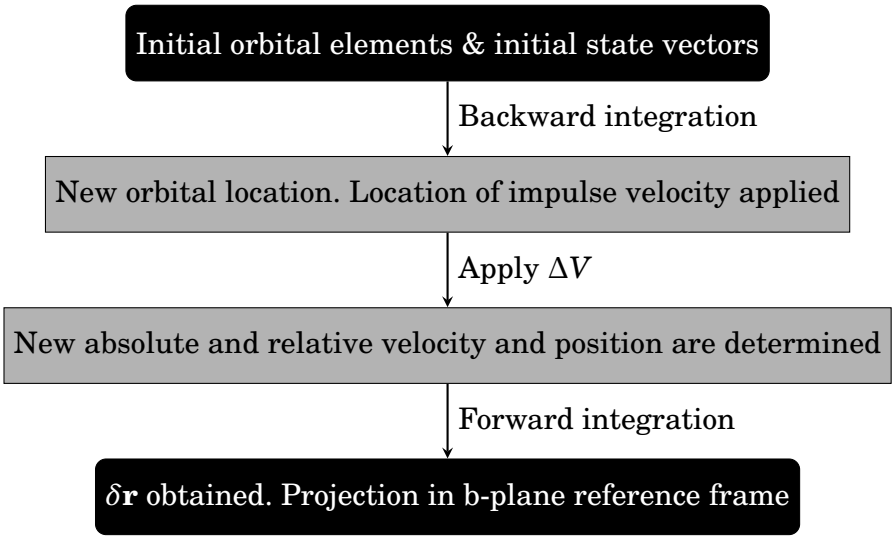

Figure 4.10: Steps followed applying relative dynamics

CHAPTER 5

CASES OF STUDY

Given the problem statement in Chapter 3 and the methodology developed in Chapter 4 it is possible to apply both of them to real cases of study. This will allow to determine the evolution of the maneuverable satellite in real examples.

This chapter is devoted to explain the cases of study in which the different methodologies have been implemented. Each of the cases of study provides the main parameters exposed in Chapter 3 which will determine the geometry of the problem.

During the project three different cases have been analysed:

- Iridium-Cosmos collision.
- Highly eccentric orbit collision.
- Near head-on collision.

The two latter cases of study are related with the main one which is the Iridium-Cosmos collision. The main parameters for each problem change as stated before, but the additional parameters, i.e. inclination, right ascension of the ascending node (RAAN) and argument of the perigee remain constant for the three cases. The three cases of study correspond to those developed in [2] in order to check the reliability of the implemented methodology and in order to compare and analyse the difference in the results.

5.1 Iridium-Cosmos collision

The Iridium-Cosmos collision is one of the most important collision events that have occurred in the last years. The collision event took place on 2009 February 10 and it involves the US communications satellite Iridium 33, which was part of the Iridium constellation of 66 satellites, and the Cosmos 2251 a Russian communications satellite that was inactive at that time. The collision was not only important in terms of the loss of the active satellite Iridium 33 but also in terms of the amount of the space debris released after the impact. The impact occurs at about 800 km altitude above Siberia (see Figure 5.1).

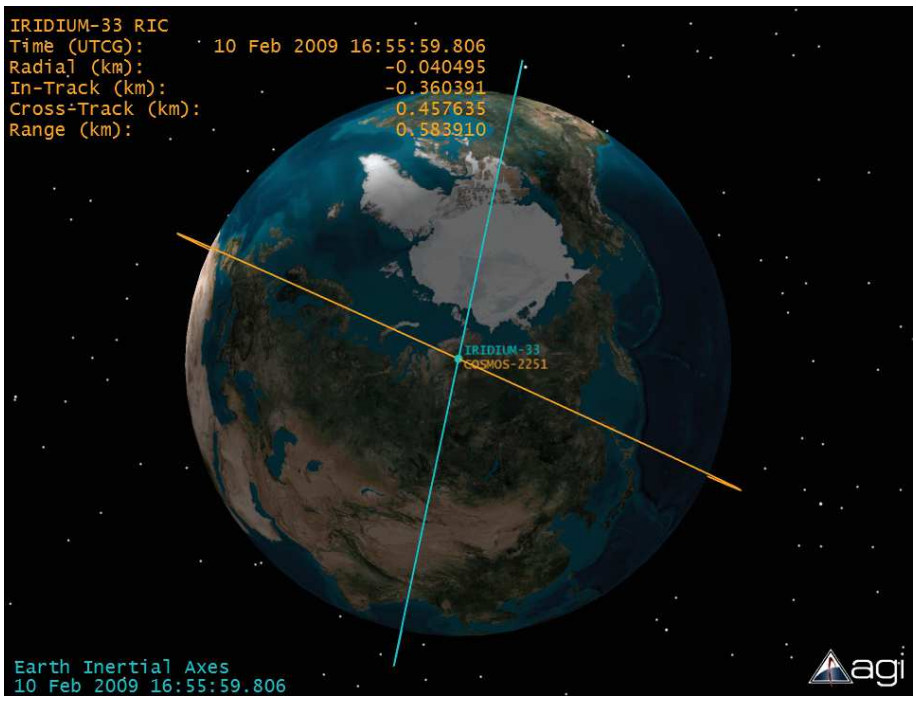

Figure 5.1: Iridium-Cosmos collision [19].

As said before, the collision was important in terms of the loss of an active satellite, Iridium 33, but also in terms of the amount of space junk released after collision. In these terms, more than 1200 space debris where released after the impact, and they suppose a threat for the current space sustainability. The collision takes place at LEO, which is the most affected area of space in terms of space junk, due to the amount of space mission launched at that orbit level. Figure 5.2 shows the space debris released after the collision impact between Iridium 33 and Cosmos 2251.

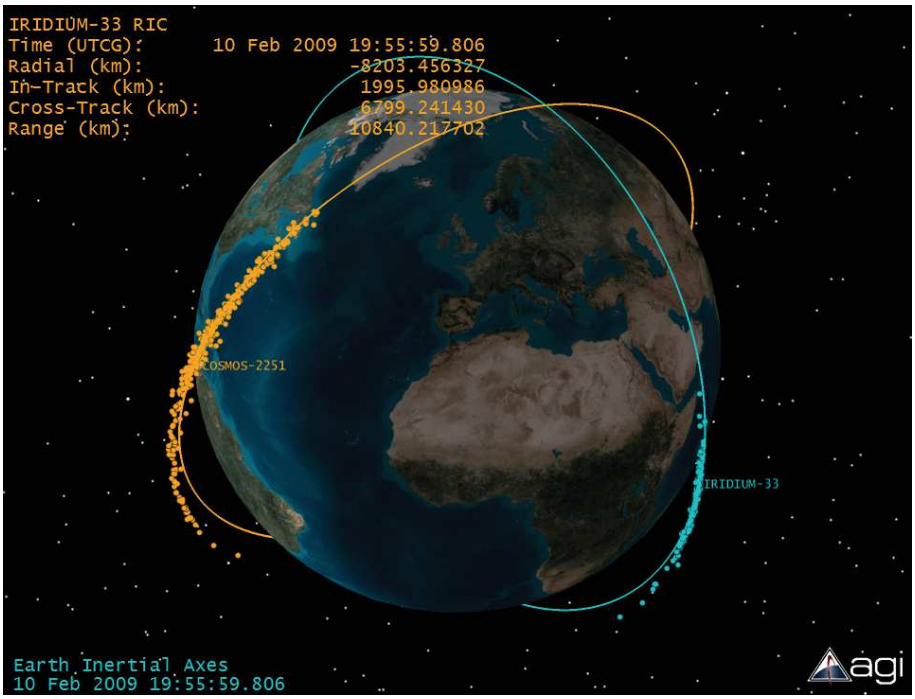

Figure 5.2: Space debris released after Iridium-Cosmos collision [19].

As this is a well-known case of collision, there are several studies which have analysed this case in other to find a solution that could have been applied. This project also covers this case of study whose main parameters are determined in [6] and can be summarized in Table 5.1.

Data	Dimensions	Value
Semi-major axis: a_0	km	7155.8
Eccentricity: e	-	2×10^{-4}
True anomaly at collision: θ_c	deg	180.0
Out-of-plane rotation angle: ψ	deg	77.5
Rotation around normal angle: ϕ	deg	-16.85
Scale factor: χ	-	1.0
Flight path angle: α	deg	0.0

Table 5.1: Iridium-Cosmos collision geometry parameters [6].

Besides the main parameters, in order to obtain a solution as close as possible to the real case, there are other parameters which determines the orbit plane that needs to be introduced. This data has been gathered from different sources [16, 19]. The information

for the orbit parameters is summarized in Table 5.2.

Data	Dimensions	Value
Inclination: i	deg	86.4
Righ ascension of the ascending node (RAAN): Ω	deg	284.6
Argument of the perigee: ω	deg	276.6

Table 5.2: Iridium-Cosmos collision geometry additional orbital parameters.

Since in this project there is not an optimization process in order to verify the reliability of the results and check them with previous studies, the parameters that need to be optimized are going to be taken from the previous project. In this sense, the parameters that are going to be taken are the in-plane rotation angle σ and the out-plane rotation angle γ shown in Figure 5.3.

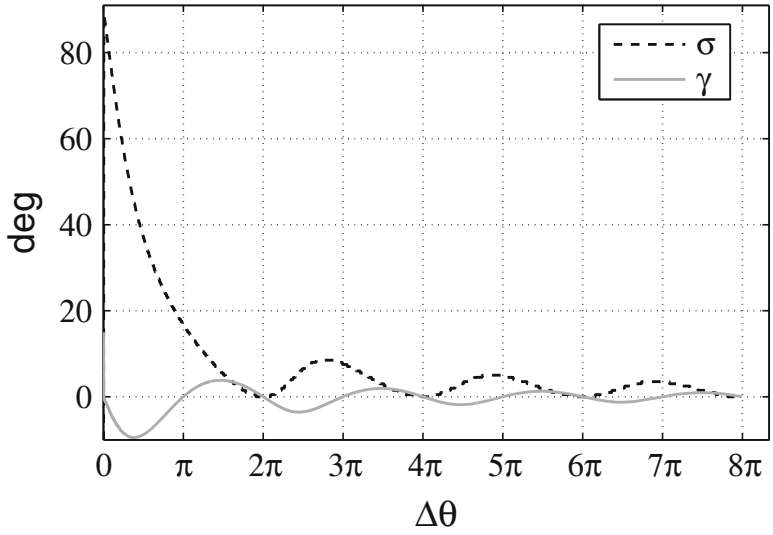

Figure 5.3: Optimal manoeuvre direction angles for Iridium-Cosmos collision [6].

Note that not the complete evolution of the manoeuvre angles is going to be gathered. The critical values associated to complete or semi periods are going to be selected to do the comparison of the results.

5.2 Highly eccentric orbit

The second case of study correspond to a highly eccentric orbit ($e = 0.95$). The collision avoidance manoeuvre is now taking into account different values for the semimajor axis a_0 as for the eccentricity.

The additional parameters in order to define the geometry of the orbit with respect to the equatorial orbit frame are the same as the ones exposed in Table 5.2 for Iridium-Cosmos collision.

Data	Dimensions	Value
Semi-major axis: a_0	km	133560.0
Eccentricity: e	-	0.95
True anomaly at collision: θ_c	deg	180.0
Out-of-plane rotation angle: ψ	deg	77.5
Rotation around normal angle: ϕ	deg	0
Scale factor: χ	-	1.0
Flight path angle: α	deg	0.0

Table 5.3: Highly eccentric orbit collision geometry parameters [6].

As for the previous case, the manoeuvre direction angles need to be determined for this case. Their evolution is observed in Figure 5.4

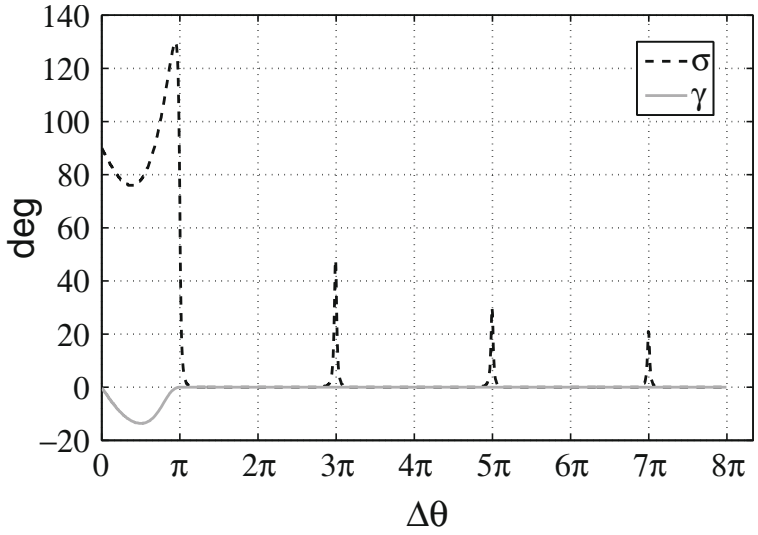

Figure 5.4: Optimal manoeuvre direction angles for highly eccentric collision [6].

5.3 Near head-on collision

The last case of study correspond to a near head-on collision between two circular orbits. The geometry of this case is gathered in Table 5.4 and the additional parameters that determine the geometry of the orbit of maneuverable spacecraft are assumed to be the same as for Iridium-Cosmos collision shown in Table 5.2. The near head-on collision is of special interest in LEO orbits where the population of satellites in orbits around 98° and 82° inclination is very high. Indeed, the Iridium 33 inclination orbit corresponds to this range of orbits. This case is also special in terms of the implementation of previous studies and it will determine the differences in the results obtained between previous studies and this project.

Data	Dimensions	Value
Semi-major axis: a_0	km	7155.8
Eccentricity: e	-	2×10^{-4}
True anomaly at collision: θ_c	deg	180.0
Out-of-plane rotation angle: ψ	deg	2
Rotation around normal angle: ϕ	deg	-16.85
Scale factor: χ	-	1.0
Flight path angle: α	deg	0.0

Table 5.4: Near head-on collision geometry parameters [6].

For this final case the manoeuvre direction angles are shown in Figure 5.5.

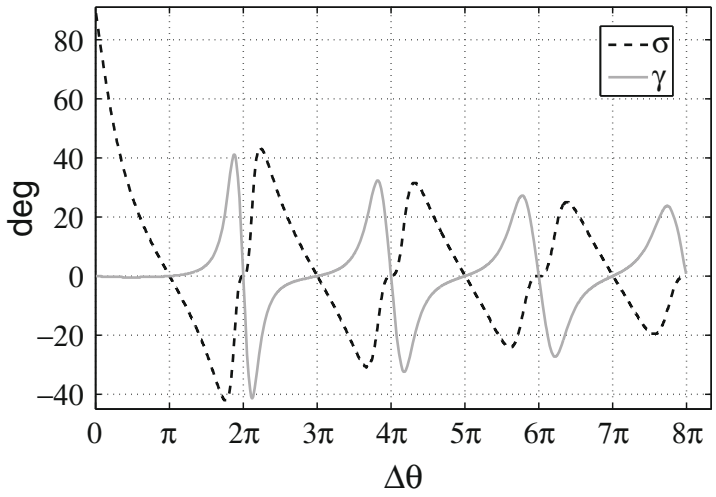

Figure 5.5: Optimal manoeuvre direction angles for near head-on collision [6].

CHAPTER 6

RESULTS

Once the problem statement, the methodology and the cases of study for this bachelor thesis have been presented, it is time to obtain the results and analyse them. This chapter is focused on the analysis and comparison of the cases of study explained in Chapter 5 taking into account the different methodologies explained in Chapter 4. The results obtained are expressed as a function of the maximum achievable miss distance for the different increment of the true anomaly of the orbit $\Delta\theta$, i.e. for different times where the manoeuvre is started.

In order to follow a similar procedure as for the methodology, the first results shown will be the associated to the Keplerian propagation and the absolute and the relative dynamics solution are presented. It is important to mention that the results for both, impulsive and low-thrust manoeuvres, are compared to the optimal manoeuvre performed in [2, 5, 6]. As said in Chapter 5 the optimization parameters are already selected regarding the ones obtained in this references. In addition, it is important to mention that the comparison of the results is made based on the characteristic parameters evolution of the optimal impulsive collision avoidance manoeuvre evolution shown in [2, 5, 6].

Each of the different methodologies will be also divided in three cases of study in order to achieve at the end of the chapter a coherent analysis between methodologies and cases of study.

6.1 Keplerian propagation

As stated in the Chapter 4, the Keplerian propagation is only applied to the impulsive collision avoidance manoeuvres. The methodology of this part of the analysis is discussed in Section 4.2.

6.1.1 Iridium-Cosmos collision

The first analysis corresponds to the Iridium-Cosmos collision. The necessary parameters are given in Tables 5.1 and 5.2.

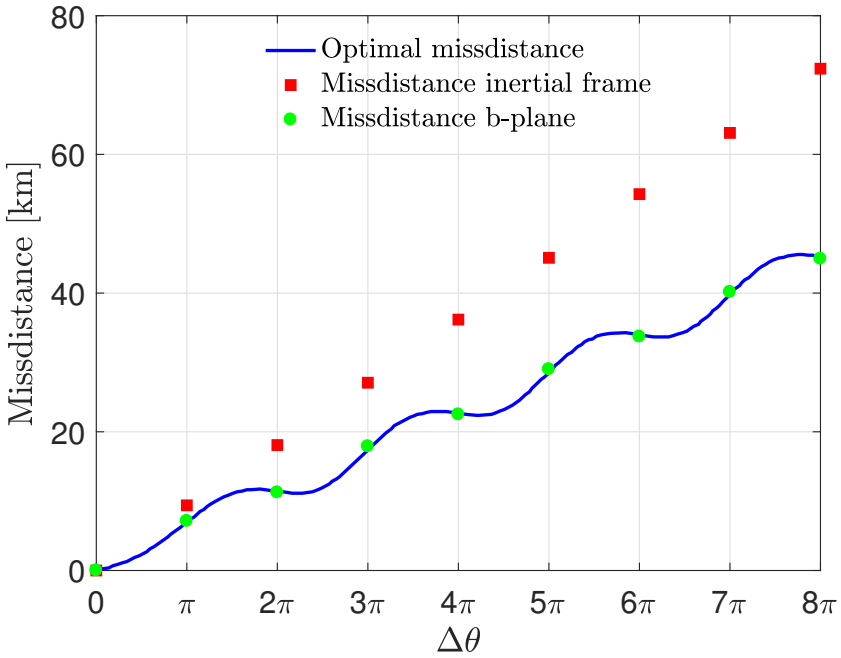

Figure 6.1: Iridium-Cosmos collision maximum miss distance [km] as a function of the manoeuvre change in the true anomaly. ΔV of 1 m/s. (Keplerian propagation)

Figure 6.1 shows the maximum achievable miss distance obtained for the Iridium-Cosmos collision problem. In the figure are presented in blue the optimal miss distance of [2, 5, 6], the miss distance obtained through the Keplerian propagation in the inertial reference frame in red, and its projection in the b-plane reference frame in green. As observed, the obtained results through the Keplerian propagation almost fit perfectly into the optimal manoeuvre evolution. The small errors are due to the gathered data for the direction manoeuvre angles (σ,γ) and for the parameters given in Table 5.2. The latter can be more significant since there is no information provided in [2, 5, 6] about

the angles that define the orbit geometry and therefore the information used for both calculations may differ in small quantities.

6.1.2 Highly eccentric orbit collision

The geometry of the second case of study is determined by Tables 5.1 and 5.2 and it corresponds to the highly eccentric orbit collision.

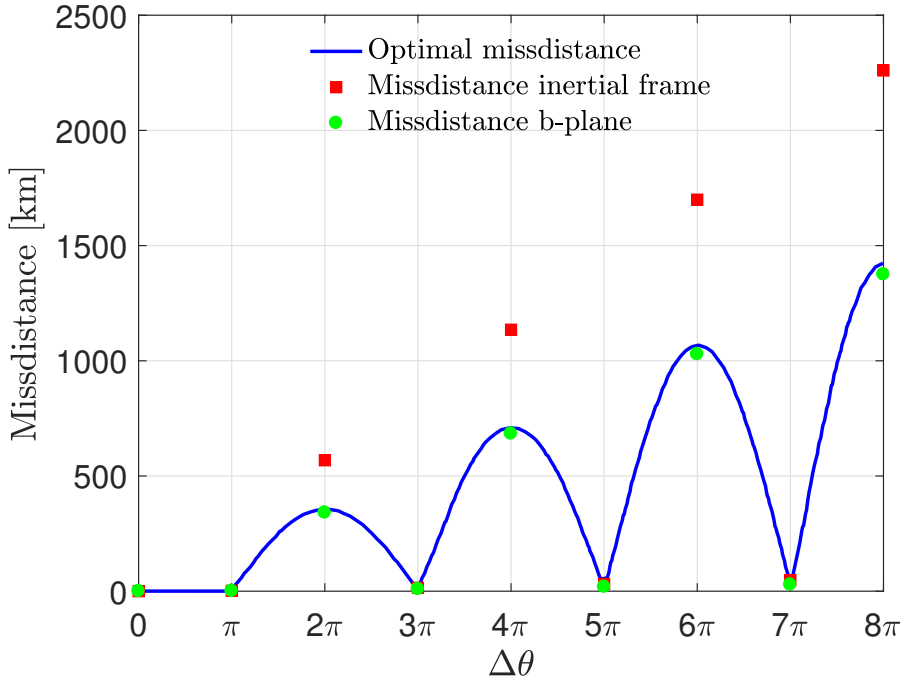

Figure 6.2: Highly eccentric orbit collision maximum miss distance [km] as a function of the manoeuvre change in the true anomaly. ΔV of 1 cm/s. (Keplerian propagation)

In Figure 6.2 in blue the optimal miss distance of [2, 5, 6], the miss distance obtained through the Keplerian propagation in the inertial reference frame in red, and its projection in the b-plane reference frame in green are presented. As for the previous case, the results in the b-plane which are the relevant once almost perfectly coincide. The small errors can be explained following a similar analysis as the exposed in the previous case of study.

6.1.3 Near head-on orbit collision

The final case of study is the near head-on collision which main parameters and geometry are defined by Tables 5.1 and 5.2. Figure 6.3 shows the evolution of the maximum

achievable miss distance being the blue line the corresponding to [2, 5, 6] works and red and blue points corresponding to the Keplerian propagation results in the inertial reference frame and in the b-plane respectively.

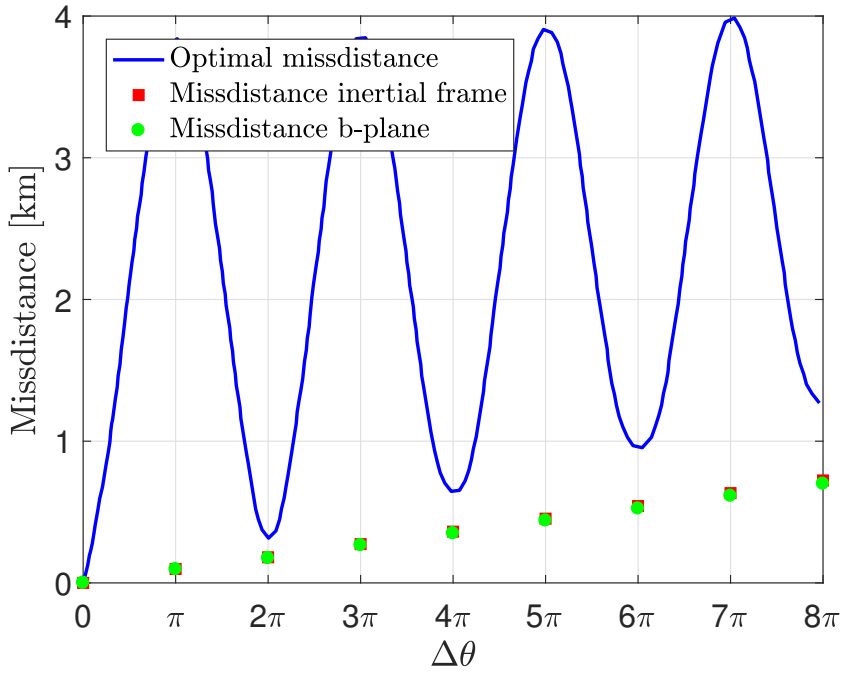

Figure 6.3: Near head-on orbit collision maximum miss distance [km] as a function of the manoeuvre change in the true anomaly. ΔV of 1 cm/s. (Keplerian propagation)

For the near head-on collision the results do not match. Although the tendency is the same, i.e. the maximum achievable miss distance increases as a function of the arc length of the collision manoeuvre $\Delta\theta$. The difference in between the data in the complete periods of the orbit can be explain doing a similar approach as for the previous cases. However, the maximum miss distance cannot be explained following the previous explanation. Since the encounter geometry of collision is different from the previous cases, due to this fact the consequent solution for the maximum achievable miss distance could have been obtained following a different approach for the Keplerian propagation. There is no clear evidence of the difference in the results and the previous arguments are hypothesis for this miss match in the solution.

As a final comment, regarding the three cases of study, the Keplerian propagation gives for two of them the almost same results that for the optimal maximum miss distance. For the third case, there are important differences at the miss distance for the half orbit periods.

6.2 Absolute dynamics

The absolute dynamics methodology is going to be applied for both, impulsive and low-thrust collision avoidance manoeuvres. The methodology of this part of the analysis is discussed in Section 4.3. In this case, the analysis is going to be divided firstly into the type of the manoeuvre and then the different cases of study are exposed. In order to repeat the previous exposed the blue line represent the optimal maximum achievable miss distance evolution from [2, 5, 6], projected in the b-plane, the red dots represent the miss distance in the inertial reference frame and the green points show the maximum miss distance projected in the b-plane (red points projected in the b-plane).

6.2.1 Impulsive manoeuvres

For the impulsive manoeuvres a velocity impulse ΔV is given at a point of the trajectory. The velocity impulse as for the previous section will be different depending on the geometry of the problem.

6.2.1.1 Iridium-Cosmos collision

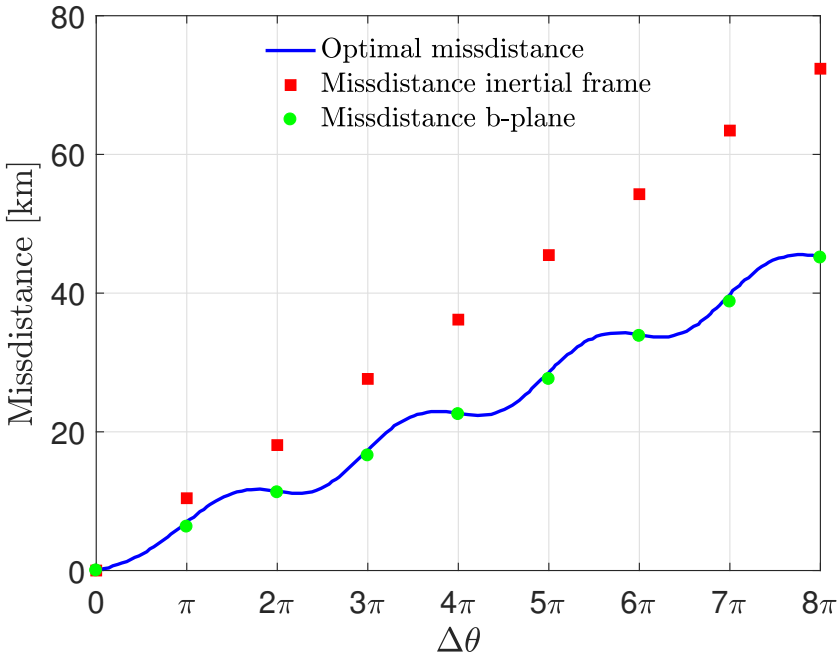

Figure 6.4: Iridium-Cosmos collision maximum miss distance [km] as a function of the manoeuvre change in the true anomaly. ΔV of 1 m/s. (Absolute dynamics)

Figure 6.4 shows the that miss distance for the absolute dynamics is almost the same as the one obtained in the optimization problem. The small difference can be explained by the difference orbit geometry taking into account for both cases, also mention in previous section and an additional contribution to the errors produced by the integration error.

6.2.1.2 Highly eccentric orbit collision

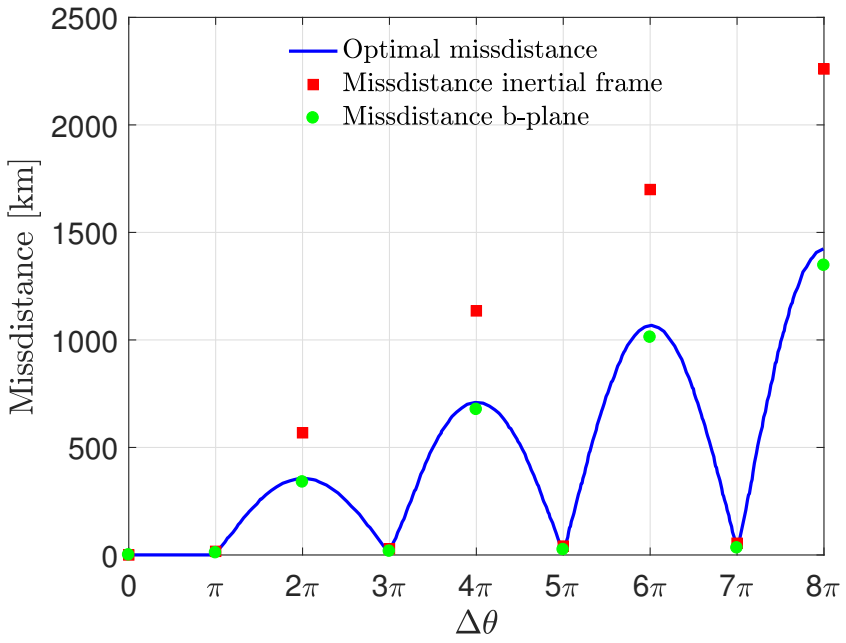

Figure 6.5: Highly eccentric orbit collision maximum miss distance [km] as a function of the manoeuvre change in the true anomaly. ΔV of 1 cm/s. (Absolute dynamics)

As for the previous case, Figure 6.5 shows an almost perfect fit between the two methodologies, in this case the errors are a bit more pronounced that in Subsection 6.1.2. The error in both evolution can be explained by doing a similar analysis as the aforementioned.

6.2.1.3 Near head-on orbit collision

The near head-on miss distance results are gathered in Figure 6.6. As for Subsection 6.1.3 the result does not match as for the previous cases. The evolution of the miss distance is conserved: it increases as a function the change in the true anomaly and it is close to the optimal results for when the satellite completes the periods. However, the difference are significant at the half periods.

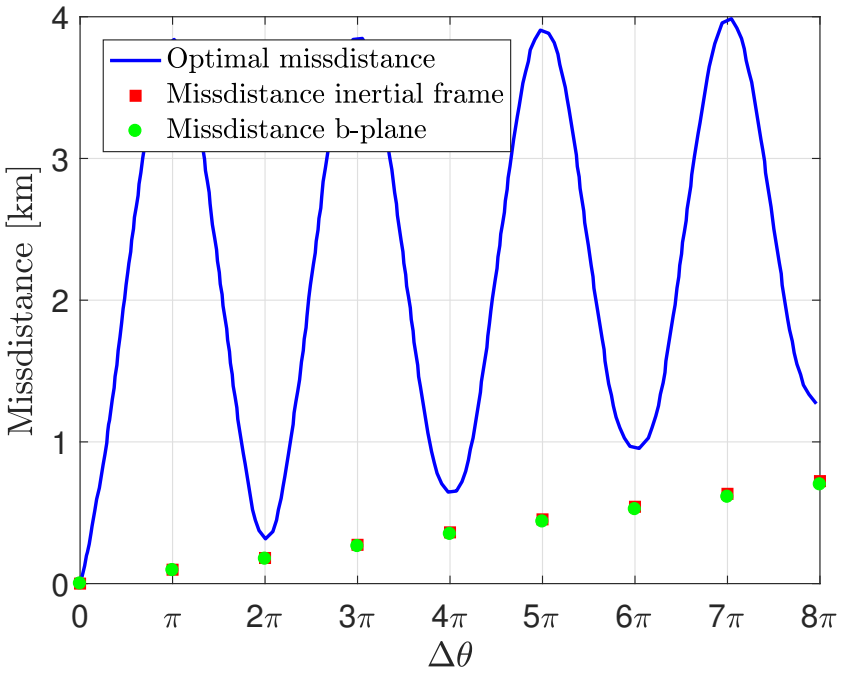

Figure 6.6: Near head-on orbit collision maximum miss distance [km] as a function of the manoeuvre change in the true anomaly. ΔV of 1 cm/s. (Absolute dynamics)

Since the results are very closed to those of Subsection 6.1.3 it can be concluded that there is a difference in the methodology, that does not take into account the encountered geometry of the problem for this case.

The miss match in the solution for this particular case and not for the others requires a further investigation in which all the assumptions made for both the optimal miss distance and the one obtained in this thesis needs to be questioned. For instance, it is the time imposed in both absolute and Keplerian propagation the same as in the optimal manoeuvre. In other words, if the time selected for the calculations is the time which gives the minimum miss distance instead of the maximum one for this particular case. This analysis can also be applied for the Keplerian propagation and relative dynamics.

6.2.2 Low thrust manoeuvres

Low thrust manoeuvres are not based on adding a velocity impulse at one point of the orbit trajectory. In this case the manoeuvre is performed through a constant thrust provided along the trajectory, i.e. from the initial point to the final one. The low thrust manoeuvres can also be done in different phases of the trajectories. For the ease of the

problem the procedure that will be implemented is the first one. The thrust provided and the mass of the satellite are based on different similar mission in LEO. In this case the mass of the maneuverable satellite is the mass of the Iridium 33 for the different cases. The Iridium 33 mass was around the 700 kg and this is the mass that is going to be used.

6.2.2.1 Iridium-Cosmos collision

For the Iridium-Cosmos collision avoidance problem there have been selected two different types of low thrust propulsion systems: one of a thrust of 50 mN and the other with a thrust of 90 mN. This values are taken based on the different types of low thrust propulsion systems that are used currently whose propellant is Xenon as NSTAR or PPS-1350.

Figure 6.7 show the different evolution for the optimal impulsive maximum achievable miss distance and the one obtained after applying low thrust to the integration. AS in the previous section, blue line correspond to the optimal impulsive case and read and green lines represent the evolution of maximum miss distance for the low-thrust problem projected in the inertial and b-plane reference frame respectively.

For case a) after it is observed that the impulsive manoeuvre is better in terms of maximum miss distance achieved. Here the thrust applied along the trajectory is 50 mN and, as stated, the mass applied is the 700 kg of Iridium 33.

However, case b) shows two different regions. On the one hand, if the manoeuvre is carried out at the closer periods to the collision event, it is shown that the impulsive manoeuvre is better. On the other hand, if the manoeuvre is performed with a great amount of time, i.e. taking the decision earlier the low-thrust manoeuvre is more efficient than the impulsive one.

In order to conclude de analysis it is important to say that the low-thrust problem is not optimized and therefore the direction in which the thrust is applied along the trajectory remains always the same, that is, does not change its direction. In the optimization problem the direction in which the thrust is applied will change the evolution of the solution and can also improve the efficiency of the low thrust manoeuvre.

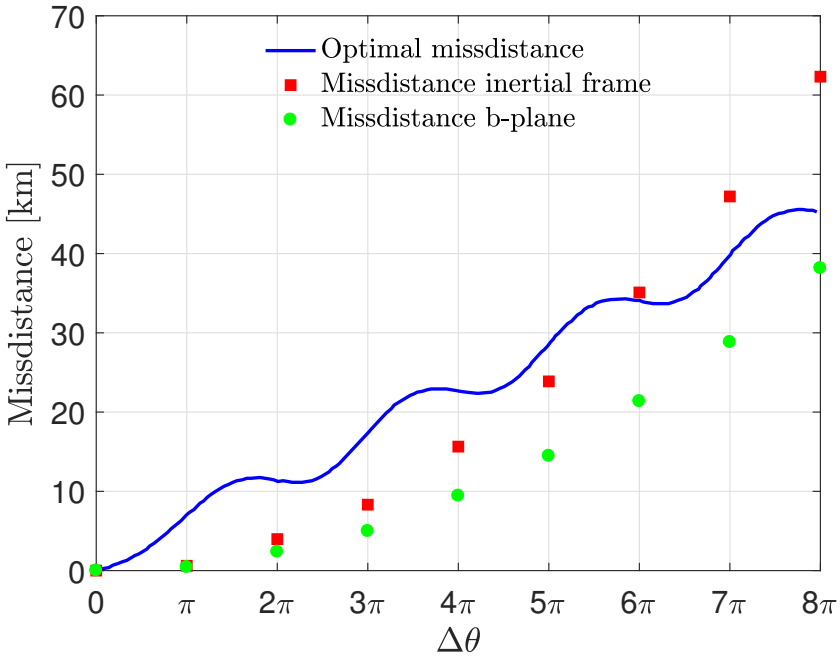

(a)

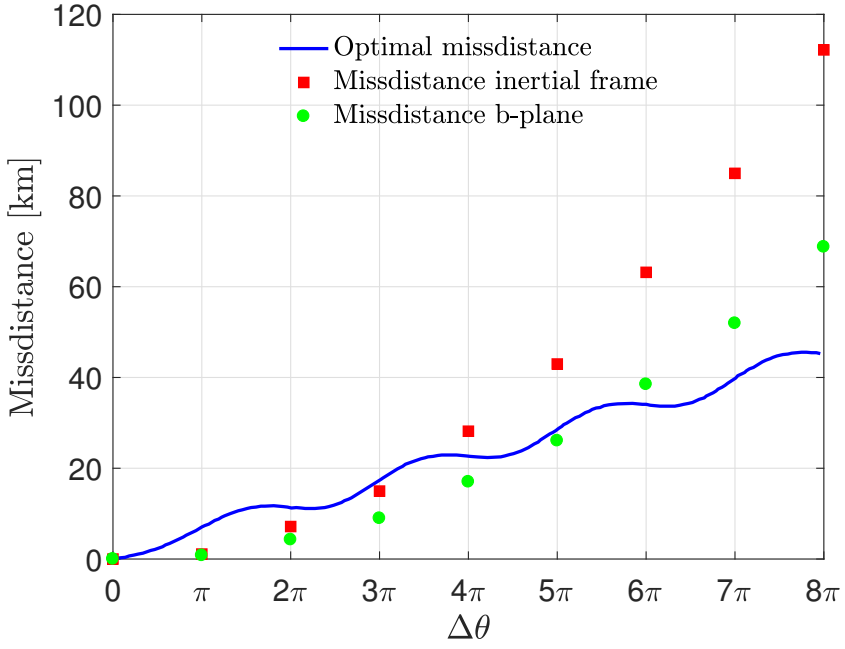

(b)

FIGURE 6.7. (a) Iridium-Cosmos collision maximum miss distance [km] as a function of the manoeuvre change in the true anomaly. T of 50 mN.(b) Iridium-Cosmos collision maximum miss distance [km] as a function of the manoeuvre change in the true anomaly. T of 90 mN.

6.2.2.2 Highly eccentric orbit collision

In this case the thrust associated to the low thrust propulsion system is 0.2 mN. This characteristic thrust is applied in some satellite to control the attitude of the satellite [22]. For this cases the propulsion system is small and the power required to control the satellite is very small.

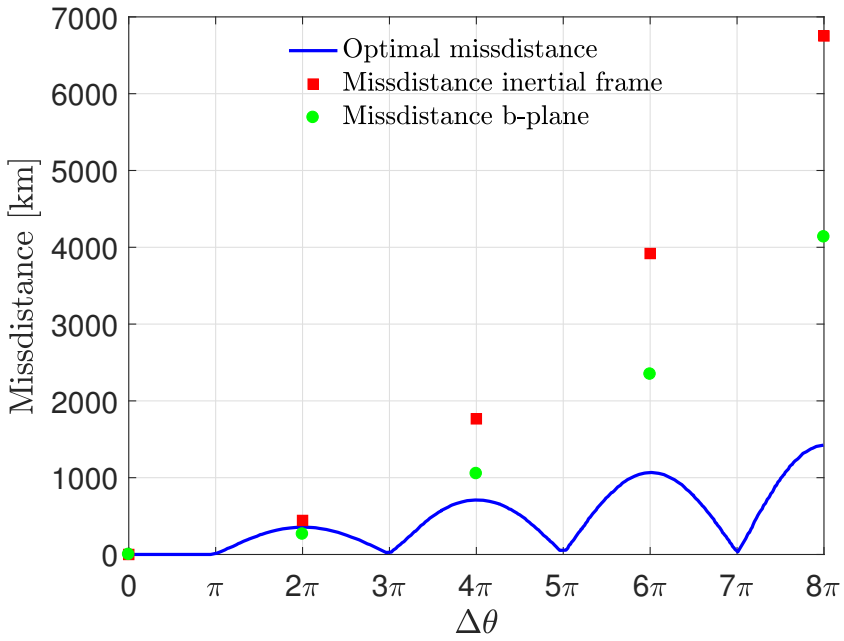

Figure 6.8: Highly eccentric collision maximum miss distance [km] as a function of the manoeuvre change in the true anomaly. T of 0.2 mN. (Absolute dynamics)

Figure 6.8 shows the evolution for highly eccentric orbit collision. Although the thrust provided by the propulsion system is very small it can be stated that is very efficient. The maximum achievable miss distance is greater for almost all the evolution of the mission. If the thrust provided would be higher the maximum achievable miss distance will be also higher. In this terms, it can be concluded that for this particular case of study the use of a low-thrust collision avoidance manoeuvre is better than carried out and impulsive one.

6.2.2.3 Near head-on orbit collision

The last case of study correspond to the near head-on orbit collision. Figure 6.9 shows the comparison between the different maximum miss distance evolution. It can be observed

that if the time of reaction to carry out the collision avoidance manoeuvre is small the impulsive manoeuvre will be the selected one. However, if the impact is detected several periods before the impact the low-thrust manoeuvre will be more efficient. Moreover, this graph shown the evolution for a provided thrust of 10 mN and therefore, if the thrust provided was higher then, the low-thrust manoeuvre would also be efficient in the times prior impact.

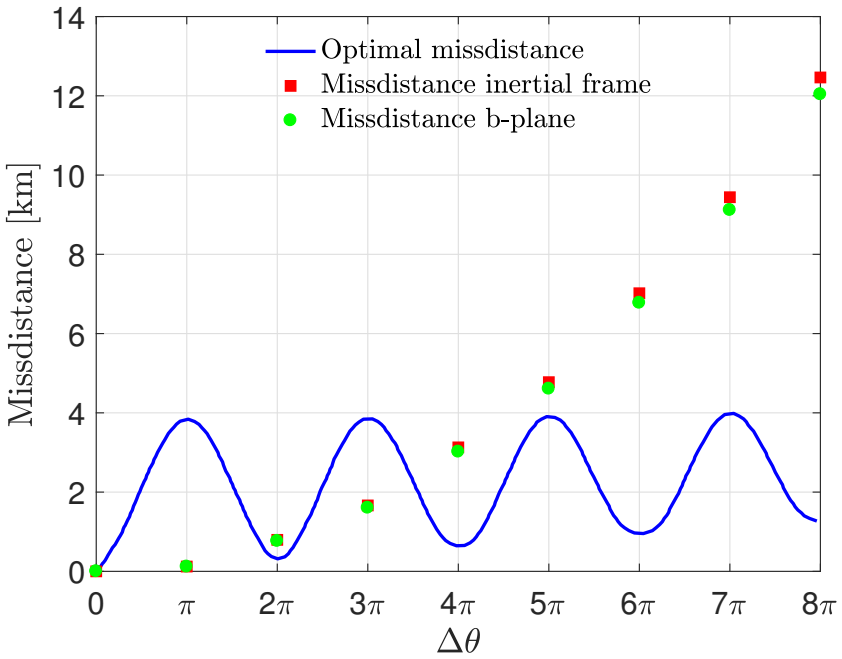

Figure 6.9: Near head-on collision miss distance [km] as a function of the manoeuvre change in the true anomaly. T of 10 mN. (Absolute dynamics)

Remembering that the low-thrust collision avoidance problem has not been optimized and, therefore, the optimal solution for the low-thrust is not achieved., but this is a good approximation for the behaviour of the evolution of the solution.

6.3 Relative dynamics

This methodology is going to be applied only for impulsive manoeuvres since the assumptions made in the methodology makes teh results for the low-thrust problem to make no sense. The formulation for the relative dynamics is developed in Section 4.4. The representation of the figures is the previously exposed.

6.3.1 Iridium-Cosmos collision

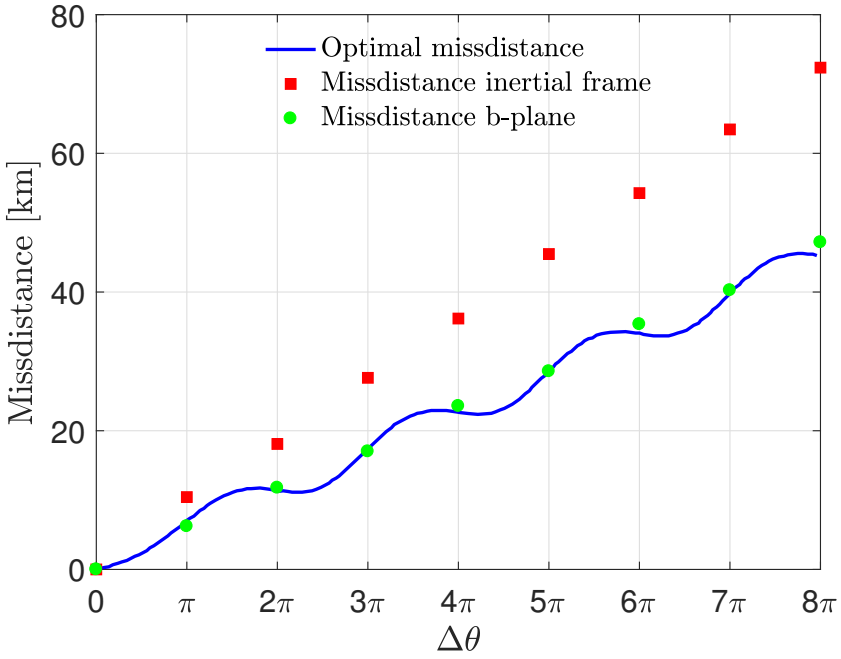

Figure 6.10: Iridium-Cosmos collision maximum miss distance [km] as a function of the manoeuvre change in the true anomaly. ΔV of 1 m/s. (Relative dynamics)

As expected Figure 6.10 shows an evolution very closed to the optimal one. There is no further commentary about the results and the comparison can be made following a similar analysis as in previous section. For some, critical points the difference are greater but they can be explained as before and due to the assumptions formulated in the methodology.

6.3.2 Highly eccentric orbit collision

As for the previous case and the same case in the other sections Figure 6.11 shows an almost perfect match between the optimal evolution of the maximum achievable miss distance and the one obtaining through the relative dynamics.

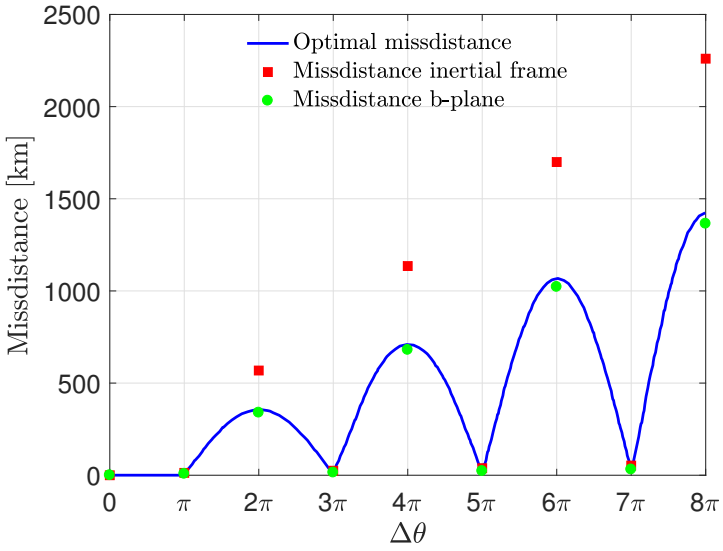

Figure 6.11: Highly eccentric orbit collision maximum miss distance [km] as a function of the manoeuvre change in the true anomaly. ΔV of 1 cm/s. (Relative dynamics)

6.3.3 Near head-on collision

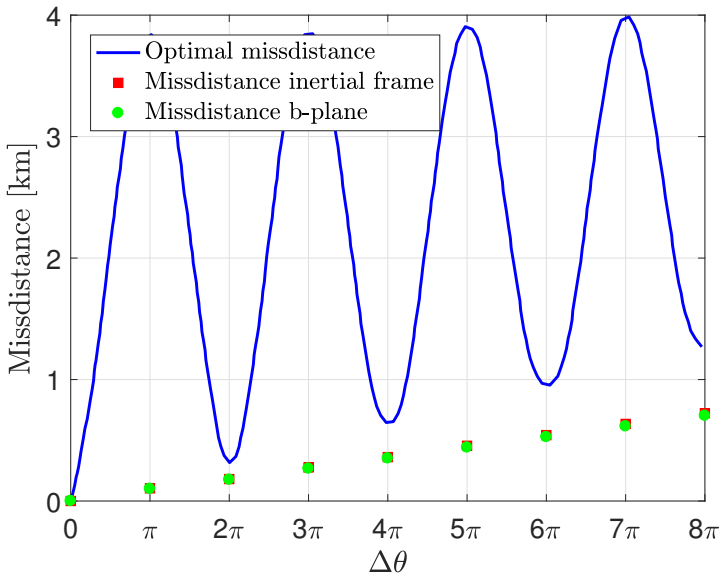

Figure 6.12: Near head-on orbit collision maximum miss distance [km] as a function of the manoeuvre change in the true anomaly. ΔV of 1 cm/s. (Relative dynamics)

The analysis explained in Subsection 6.2.1.3 which applies for the difference between optimal and the obtaining solution of the evolution of the maximum miss distance can be also explained the differences of this part.

CHAPTER 7

FUTURE WORK

After the complete analysis and discussion of the results for the study cases in which the different methodologies have been applied it is also important to consider the possible future work of this project. This chapter is dedicated to expose the possible branches of study that can be developed taken as a base the present project. Some of them was considered to be developed through this project but it could not be possible to carry out them.

- This thesis covers different methodologies different from the ones that have been previously studied. In this sense, the problem has not been optimized and the optimization parameters has been taken from the previous studies with different methodologies. In order to be accurate with the methodology of the project an optimization process can be implemented. The results of the optimization will give the optimal maximum miss distance produced by the collision avoidance manoeuvre. The parameters that optimize the solution (σ,γ) are going to be optimize and their evolution will be able to be determined.

- Additional effects to the collision avoidance problem can be implemented. In real and no ideal case there are perturbations and additional forces that act over the problem. In this project the contribution of this perturbations are neglected but they can be accounted. For instance, the effect of $J2$ can be implemented in the code by changing the equations of the methodology in order to define a more realistic model of the problem.

- The problem can be developed for different missions and varying the parameters. For instance, the equations determined in this problem can be used to solve different problem as the CryoSat exposed in Chapter 2. Another different case of study that can be implemented is the last collision avoidance manoeuvre performed by the ESOC, the Swarm-B collision avoidance manouevre. Although the propulsion subsystem of the satellite is based on cold gas propulsion, and hypothesis about the implementation of low-thrust propulsion system can be made and, therefore, the analysis for the real data and the idealise data with the low-thrust assumption can be made in order to observe the advantages and disadvantages of it.

- Another future work is to evaluate the effect of the shadow and pre-shadow in the maneuverable satellite. These effects affect the satellite power system and, therefore, also vary the velocity impulse that can be provided depending on the location of the satellite.

- As a final point, it could also be mentioned the studied applied not only for the point of one collision but for the case of multicollision with different space debris. In this case, the objective would be to try to optimize the direction of the collision avoidance manoeuvre to avoid the collision with different space debris and optimizing the maximum missdistance for both space debris.

CHAPTER 8

CONCLUSIONS

The final chapter of the bachelor thesis corresponds to the conclusion. In this chapter, all the goals achieved and the knowledge learnt are going to be summarized. And also a special mention regarding a general overview of the project is going to be carried out.

During the development of the thesis the main goals of Section 1.5 have been achieved. One of the more important parts of the thesis has been the research of information to obtain a general view of the collision avoidance problem. Moreover taking into account that the formulation of the problem was stated in complex parameters, the first is step of understanding the information has been difficult.

Once the main general concepts and the problem statement of the problem was stated it has to be applied to the specific formulation developed during this thesis. In this sense, the main concepts of absolute and relative dynamics in space have been learnt and applied to the problem of collision avoidance manoeuvres. In addition, in order to clarify the concepts related with motion in space the Keplerian propagation was proposed and finally carried out. This has allowed to get a further knowledge to this topics.

Since this is not a new branch of study, the problem has also several backwards. For instance, the reliability of the results is subjected to previous analysis and results. On the other hand, the use of previous information and documentation allows to have a

more critical perspective on the results obtained.

To sum up, during the fulfilment of the current bachelor thesis the problem of collision avoidance manoeuvres has been researched, studied and analysed. This analysis has been taken into account the problem with space sustainability and also regarding the utilisation of new low-thrust propulsion system. The problem has been researched in taking into account the impulsive optimal solution and the present document has tried to go deep in this analysis but also trying to implement the low thrust solution for the problem. Since both solutions have been developed, obtaining results for both solution prior their analysis and comparison has been made. Therefore, the thesis has gone trough the methodology, cases of study, formulation and results related to the collision avoidance problem trying to get the low-thrust solution as the most innovative part of the project.

BIBLIOGRAPHY

[1] M. R. AKELLA AND K. T. ALFRIEND, *Probability of collision between space objects*, Journal of Guidance, Control, and Dynamics, 23 (2000), pp. 769–772.

[2] C. BOMBARDELLI, *Optimal impulsive collision avoidance*, Optimal Impulsive Collision Avoidance, 148 (2013), pp. 1–17.

[3] C. BOMBARDELLI, G. BAÙ, AND J. PELÁEZ, *Asymptotic solution for the two-body problem with constant tangential thrust acceleration*, Celestial Mechanics and Dynamical Astronomy, 110 (2011), pp. 239–256.

[4] C. BOMBARDELLI AND J. HERNANDO-AYUSO, *Optimal impulsive collision avoidance in low earth orbit*, Journal of Guidance, Control, and Dynamics, 38 (2015), pp. 217–225.

[5] C. BOMBARDELLI, J. HERNANDO-AYUSO, AND R. GARCÍA-PELAYO, *Collision avoidance maneuver optimization*, Advances in the Astronautical Sciences, (2014), pp. 214–335.

[6] C. BOMBARDELLI, *Analytical formulation of impulsive collision avoidance dynamics*, Celestial Mechanics and Dynamical Astronomy, 118 (2014), pp. 99–114. http://dx.doi.org/10.1007/s10569-013-9526-3.

[7] F. K. CHAN, *Spacecraft collision probability*, Aerospace Press El Segundo, CA, 2008.

[8] COMMITTEE ON THE PEACEFUL USES OF OUTER SPACE. SCIENTIFIC AND TECHNICAL SUBCOMMITTEE, *Guidelines for the long-term sustainability of outer space activities*, (2017). http://www.esa.int/spaceinimages/Images/2017/04/Draft_UN_guidelines.

[9] H. D. CURTIS, *Orbital Mechanics for Engineering Students (Third Edition)*, Butterworth-Heinemann, Boston, third edition ed., 2014.

http://www.sciencedirect.com/science/article/pii/B978008097747801001X.

[10] ESA Space Debris Office, *Esa's annual space environment report*, tech. rep., European Space Operation Centre, April 2017.
https://www.sdo.esoc.esa.int/environment_report/Environment_Report_I1R2_20170427.pdf.

[11] European Space Agency, *Reentry and collision avoidance*, April 2017.
http://www.esa.int/Our_Activities/Operations/Space_Debris/Reentry_and_collision_avoidance.

[12] Federal Aviation Administration, *Commercial space and launch insurance: Current market and future outlook*, tech. rep., Federal Aviation Administration, Fourth Quarter 2002 Quarterly Launch Report, 2002.
https://www.faa.gov/about/office_org/headquarters_offices/ast/media/q42002.pdf.

[13] P. Gavigan, *Estimation of minimum required thrust for spacecraft collision avoidance*, (2013).

[14] Gobierno de España, *Disposición 542 del BOE núm. 15 de 2017*, Ministerio de la Presidencia, January 2017.
https://www.boe.es/boe/dias/2017/01/18/pdfs/BOE-A-2017-542.pdf.

[15] M. Graziano, F. Pirondini, N. Sánchez, and E. Di Sotto, *Cryosat collision warning and low thrust avoidance manoeuvre strategy*, in Space Debris, vol. 473, 2001, pp. 455–461.

[16] Heavens Above, *Iridium 33 - órbita*, June 2017.
http://www.heavens-above.com/orbit.aspx?satid=24946&lat=0&lng=0&loc=Unspecified&alt=0&tz=UCT.

[17] Inter-Agency Space Debris Coordination Committee and others, *Iadc space debris mitigation guidelines*, (2007).
http://www.iadc-online.org/Documents/Docu/IADC_Mitigation_Guidelines_Rev1_Sep07.pdf.

[18] N. L. JOHNSON, E. STANSBERY, D. O. WHITLOCK, K. J. ABERCROMBY, AND D. SHOOTS, *History of on-orbit satellite fragmentations*, tech. rep., NASA Johnson Space Center; Houston, TX, United States, May 2008.
https://ntrs.nasa.gov/search.jsp?R=20080022435.

[19] T. KELSO ET AL., *Analysis of the iridium 33-cosmos 2251 collision*, Advances in the Astronautical Sciences, 135 (2009), pp. 1099–1112.

[20] E. M. LEVIN AND J. A. CARROLL, *The cost of future collisions in leo*, White Paper, February, 28 (2012).

[21] C. LOUEMBET AND G. DEACONU, *Collision avoidance in low thrust rendezvous guidance using flatness and positive b-splines*, in American Control Conference (ACC), 2011, IEEE, 2011, pp. 456–461.

[22] S. MARCUCCIO, A. GENOVESE, AND M. ANDRENUCCI, *Experimental performance of field emission microthrusters*, Journal of Propulsion and Power, 14 (1998), pp. 774–781.

[23] M. MASSARI AND F. BERNELLI-ZAZZERA, *Optimization of low-thrust reconfiguration maneuvers for spacecraft flying in formation*, Journal of Guidance, Control, and Dynamics, 32 (2009), pp. 1629–1638.

[24] A. MAZZOLENI, M. LUENGO, J. A. SANTOS, A. ITURRI, I. BUENO, P. PISABARRO, AND F. PIRONDINI, *Collision avoidance operations of deimos-1 and deimos-2 missions*, in 14th International Conference on Space Operations, 2016, p. 2450.

[25] D. OLIVIERO AND M. SANJURJO-RIVO, *A parametric study on leo collision avoidance manoeuvres*, (2015).

[26] J. PELÁEZ, J. M. HEDO, AND P. R. DE ANDRÉS, *A special perturbation method in orbital dynamics*, Celestial Mechanics and Dynamical Astronomy, 97 (2007), pp. 131–150.

[27] H. SCHAUB AND J. L. JUNKINS, *Analytical mechanics of space systems*, Aiaa, 2003.

[28] D. SCUKA, *Taking action at esoc*, January 2017.
http://blogs.esa.int/rocketscience/2017/01/24/taking-action-at-esoc/.

[29] G. VALSECCHI, A. MILANI, G. GRONCHI, AND S. CHESLEY, *Resonant returns to close approaches: Analytical theory*, Astronomy & Astrophysics, 408 (2003), pp. 1179–1196.

[30] B. WU, D. WANG, AND E. K. POH, *Energy-optimal low-thrust satellite formation manoeuvre in presence of j 2 perturbation*, Proceedings of the Institution of Mechanical Engineers, Part G: Journal of Aerospace Engineering, (2011), p. 0954410011408659.